SOLAR COLLECTION LIMITATIONS FOR DYNAMIC CONVERTERS
Simulation of Solar-Thermal Energy Conversion Systems*, **

by

George L. Schrenk

University of Pennsylvania, Philadelphia, Pennsylvania

and

Consultant, Allison Division G.M.C., Indianapolis, Indiana

ABSTRACT

A mathematical model for analysis of actual solar collectors has been developed. This model allows one to calculate the energy flux on any arbitrarily shaped focal surface from any arbitrarily shaped collector surface without making numerical approximations. Provisions are included for treating random surface errors on the reflector surface, orientation errors of any size, and vignetting of reflected light by a cavity opening. Typical results from this model are presented to show the effects of surface and orientation errors.

This model has recently been used to investigate the interface between the collector and the heat receiver—the cavity opening. The directional assumption ordinarily made for this interface is that this opening can be treated as if it were a plane surface that emitted radiation according to Lambert's law (i.e., the cosine law). Results are presented that clearly show that this assumption is in substantial error for both perfect and imperfect collectors.

Detailed analytical work has been performed on cylindrical heat receivers coupled with typical collectors. An "open cavity" Fredholm integral equation approach and the valid directional distribution have been utilized. The effects of the absorptivity and emissivity of the walls of the heat receiver have been investigated; reradiation losses and system performance have been calculated. The results presented differ significantly from the usual engineering estimates used in the design of solar power systems.

---

*This research was supported in part by Allison Division G.M.C. and in part by NASA ~~Contract~~ Grant NsG-316 to the Institute for Direct Energy Conversion of the Towne School of Civil and Mechanical Engineering of the University of Pennsylvania.

**This paper was presented at the AGARD Conference held in Cannes, France, March 16-20, 1964.

INTRODUCTION

Fundamental to the analysis of solar reflectors is the fact that the source (sun) is not a point source. Because of this fact the classical techniques of ray tracing no longer apply to describe the energy distribution and its conversion. Instead, cone tracing techniques must be used—as a cone can be used to represent the light coming from a small but finite source. The concept of cone tracing was introduced by F. Cabannes and A. Le Phat Vinh (1)* in 1954 and by N. Hukuo and H. Mii (2) in 1957. Cabannes and Le Phat Vinh considered only perfect paraboloids. Hukuo and Mii also considered perfect paraboloids, but they then attempted to apply their results to real reflectors by introduction of a "scattering circle" concept—i.e., the reflected cones are statistically scattered in the focal plane uniformly over a circular region.

Hukuo and Mii were perhaps the first to apply statistics to predict real reflector performance by introducing the "scattering circle" concept. This concept was extended to the use of a normal distribution in the focal plane (in place of the uniform distribution of the "scattering circle" concept) by various individuals late in 1960 (3, 4) and several papers have since been published on this by other authors (5, 6). It is important to point out that this concept applies a probability distribution to a scattering of points in the focal plane; thus, it is not possible to relate theoretically the probability distribution in the focal plane with the surface contour errors due to the manufacturing procedures on the reflector surface. The alternative is to apply the probability distribution to the surface normals on the reflector. Physically, this is the most desirable and meaningful approach; however, it is also the most difficult to implement. Perhaps the first person to try this type of approach was Silvern (7). His work, however, was burdened with several errors and numerous significant approximations. He assumed that finite rotations commute (i. e., he assumed that the sum of finite rotations does not depend on the order of the rotations) and he applied the normal distribution function incorrectly to angles. He did, however, obtain numerical results from his work. Since this time, in addition to the work discussed here, there have been several other attacks on this problem. Fuller (8) formulated a mathematical approach to this problem. His work, however, suffers from several major problems: (*i*) he applied the normal distribution function incorrectly to angles, and (*ii*) his work was never successfully programmed on a computer. General Electric (9) has also carried out analytical work to predict the performance of a reflector possessing a fixed specific surface error over the entire surface. No provisions were made to treat orientation errors and no introduction of statistics was made. General Electric, however, did achieve operative computer programs.

---

*Numbers in parentheses refer to references listed at the end of this paper.

Theoretical work on optical analysis problems was started by this writer (under contract to Allison Division G.M.C.) early in 1959. Initially cone tracing techniques were used to analyze conical serration Fresnel reflectors. This work, however, was restricted to perfect surfaces. Upon completion of this work (10, 11) in late 1960, work was started toward the analysis of actual solar reflectors.

From the start, the required model of a solar collector had to be as general as possible and had to be capable of analyzing both perfect and imperfect (actual) reflectors. Because of the necessary complexity of such a general model, from the very first the goals of this work were twofold:

i. Development of a mathematical model

ii. Development of an operative computer program from this mathematical model.

The many problems encountered can be appreciated by reference to the interim report (12), written in June, 1961. Over a period of time the desired mathematical model for actual solar collectors (13, 14, 15) was successfully developed. This model included provisions for treating random surface errors on the reflector surface and orientation errors of any size. Furthermore, almost all the approximations introduced by others into cone optics were removed. The approach to the development of the mathematical model was judiciously selected to result in a practical and useful tool for the design and evaluation of solar-thermal energy conversion systems. The operative computer program (D70E) for evaluating solar reflectors that was developed from these equations is practical and feasible from a computational (and computer running time) viewpoint.

Although the mathematical model is applicable to any conceivable reflector, the computer program (D70E) was designed to treat only paraboloidal reflectors, conical Fresnel serrations, spherical Fresnel serrations and/or any part of these reflectors. This initial work, however, was restricted to the determination of the magnitude of the energy distribution on any plane surface perpendicular to the optical axis.

In early 1963, a copy of this D70E program was purchased by Aerospace Corp. (under contract No. 62-167) to be used as part of a complete solar-thermal energy conversion system computer program under development there. As already pointed out, the only restriction in this work to date was that it applied only to plane focal surfaces. Although the use of plane focal surfaces is convenient for a general study of solar reflectors, the results obtained are <u>not</u> in a convenient form for use in connection with the analysis of a solar-thermal energy absorber, such as a cavity. In fact, the use of

such results requires that critical assumptions be made concerning the directional distribution of the energy flux in the focal plane. Because of this, Aerospace found it highly desirable to extend the previous analytical work to be able to calculate the energy flux distribution on any arbitrarily shaped focal surface (e.g., a cavity wall). With this extended capability, the mathematical model would then not only check the directional assumptions used, but would also obviate the need for making any directional assumptions. The perfection of such a generalized mathematical model would provide the solar power system designer with mathematical tools that were heretofore unavailable.

This extended mathematical model was developed and perfected at Allison under contract AF-04(695)-335. As a result of this extended work, all the approximations introduced into cone optics have been removed; it is now possible to calculate the energy flux distribution on any arbitrarily shaped focal surface from any arbitrarily shaped reflector surface. This model includes provisions for treating random surface errors on the reflector surface, orientation errors of any size, and vignetting* of reflected radiation by a cavity opening. No approximations are introduced; the model is accurate within the limitations of the numerical techniques of integration on high speed digital computers. An operative computer program (74 B) for evaluating solar reflectors has been developed from this theoretical work; this program is practical and feasible from a computational (and computer running time) viewpoint (15).

---

*The term vignetting refers specifically to blockage of reflected light by a cavity opening. This is in contrast to the term blockage, which is used to refer specifically to blockage of incident light on the reflector. In addition to vignetting, provisions also exist for treating blockage of incident light.

SOLAR REFLECTOR MODEL*

The broad scope and generality of this mathematical model of a solar reflector can readily be seen from the following outline of the input parameters:

Mathematical Solar Simulator

- Source Parameters
  - Solar half angle
  - Source type
    - Uniform
    - Limb darkening
- Reflector Parameters
  - Arbitrarily shaped reflector surface** including blockage effects
- Surface Parameters
  - Perfect reflector surface
  - Imperfect reflector surface (errors of all sizes)
    - One-dimensional normal distribution applied to the surface normals
    - Two-dimensional normal distribution applied to the surface normals
- Orientation Parameters
  - Orientation errors of all sizes
- Vignetting Parameters
  - Circular hole vignetting
    - Arbitrary position, size, and orientation of opening
- Focal Surface Parameters
  - Arbitrarily shaped focal surface

A detailed description of this mathematical model of a solar reflector is beyond the scope of this paper. A complete description of this model and its accompanying computer programs is given in reference 15.

The power of this mathematical solar simulator can best be seen by examination of some typical results. For the purpose of this paper, let us consider only paraboloidal reflectors, as illustrated in Figure 1. We shall always choose $R = 1.0$ for the sake of normalization.

*The terms reflector and collector are used interchangeably throughout this paper; likewise, the terms heat receiver and cavity.

**Although the theory applies to any arbitrarily shaped reflector surface, the computer programs are presently designed to treat paraboloidal reflectors, conical Fresnel serrations, spherical Fresnel serrations and/or any part of these reflectors. (The energy flux distribution from a Fresnel reflector is the sum of the energy flux distributions of the individual serrations.)

Let us first consider only plane focal surfaces, perpendicular to the principal axis of the reflector and intersecting the principal axis at the point source focus. Let the source be a uniform disk subtending a half angle of $\alpha' = .00465$. Let

σ_x = circumferential standard deviation of the surface normal

σ_y = radial standard deviation of the surface normal

I = concentration ratio of reflected light. Multiplication of I by the solar constant and the coefficient of reflection results in the actual energy flux/unit area incident on the focal surface point.

β = polar orientation angle between the central ray from the sun and the principal axis of the reflector

$\eta_{collection}$ = power collected in area πr^2 / total power reflected from the reflector*

Figure 2 shows results as a function of rim angle for $\sigma_x = \sigma_y = 0$, $\beta = 0$. Figure 3 shows results for a 60° paraboloidal reflector as a function of β for $\sigma_x = \sigma_y = 0$. Figures 4, 5, 6, 7 show results for a 60° paraboloidal reflector as a function of surface errors for $\beta = 0$. These results are presented here as typical examples of the use of this mathematical solar simulator for plane focal surfaces. These results are self explanatory and will not be discussed further.

Plane focal surface results have been used in the past as a means of comparing various reflectors and optimizing reflector designs. The validity of this approach, however, is now dubious. This approach was based on the premise that the prediction of the performance of the heat receiver could effectively be isolated from the reflector. More specifically, it was usually assumed that reradiation losses from the heat receiver could be calculated as if the cavity opening were a simple gray body. The reflector design was then optimized on the basis of this simple prediction of reradiation losses.

Recently, detailed calculations of heat receiver performance have shown that the assumption that the cavity opening can be considered as if it were a simple gray body is incorrect. In fact, the reradiation losses are usually much greater, as will be seen later on in this paper (Figures 15, 16). Thus, the optimization of the reflector design can no longer be considered independent of the cavity; instead, they must be optimized as a system. Detailed calculations of the heat receiver performance are essential.

---

*Total power reflected from the reflector = (coefficient of reflection)x(total power incident on the reflector); r denotes the focal plane radius, as shown in Figure 1.

REFLECTOR-CAVITY INTERFACE

Now, in the detailed prediction of cavity performance another question arises that makes the usefulness of plane focal surface results even more dubious. In order to calculate the performance of the cavity, it is necessary to know the energy flux distribution on the walls of the cavity. Before the development of this extended mathematical model (15), it was not possible to calculate this energy flux distribution directly. Instead, it was necessary to take plane focal surface results and make a crucial assumption about the directional distribution of the radiation entering the cavity. The directional assumption ordinarily made (16, 17) is that the cavity opening can be treated as if it were a plane surface that emitted radiation according to Lambert's Law (i.e., the cosine law). Thus, the predicted energy flux on plane focal surfaces was used—via Lambert's Law—to calculate the solar energy flux incident on the walls of the cavity. Clearly this type of approach still tends to isolate the study and design of the cavity from that of the reflector, although to a lesser degree than the simple gray cavity approach.*

With the recent perfection of the generalized mathematical model (described in reference 15), it is now possible for the first time to investigate this assumption. This question can be investigated in two ways. First, the actual directional distribution can be calculated. This is best done by looking at a hemispherical cavity with a small opening located on the principal axis of the reflector. Second, the actual energy flux incident on the walls of typical cavities can be calculated and compared with similar results obtained through the use of Lambert's Law. This tells how important any deviations from Lambert's Law will be for any proposed cavity configuration. Figure 3 shows a sketch of the hemispherical cavity used to determine the directional distribution and the cylindrical cavity used to examine the importance of deviations from Lambert's Law for a typical cavity.

For a perfect reflector ($\sigma_x = \sigma_y = 0$) Figure 9 shows a plot of I versus cos θ for the hemispherical cavity of Figure 3. Figure 9 also shows a polar plot of these results that clearly shows the directional distribution. Figure 11 shows a plot of I along the walls of the cylindrical cavity for $z/d = 1, 2, 3$. The opening of this cavity was arbitrarily chosen so that the cavity collected 90% of the reflected energy. Lambert's Law has also been plotted in these figures for the purpose of comparison.

The same results have been obtained for a typical imperfect 60° paraboloidal reflector with $\sigma_x = 5'$, $\sigma_y = 10'$. Figure 10 shows a plot of I versus cos θ for the same hemispherical cavity and a polar plot of these results to show the directional distribution. Figure 12 shows a plot of I along the walls of the cylindrical cavity for $z/d = 1, 2, 3$. Here, also, the cavity opening was arbitrarily chosen so that the cavity collected 90% of the reflected energy. Lambert's Law has also been plotted in these figures for the purpose of comparison

* Another assumption occasionally made is that the energy flux distribution on a spherical surface is uniform (19). Results shown in Figures 9 and 10 readily show that this assumption is in substantial error.

The results shown in Figure 12 contain some interesting "fine structure" effects—specifically the peaking of I on the back wall of the cylinder as $x \to 0$ (i.e., as we approach the principal axis of the reflector). Figure 11, however, shows that this peaking is not present in perfect reflectors. A detailed study of this effect has shown that this peaking is purely a statistical effect. Figure 13 shows a histogram of the number of reflector areas versus probability for $z = .06$, $x = .012$ and for $z = .06$, $x = 0$. This histogram shows that as $x \to 0$, the number of reflector areas that have large probabilities associated with them increases, thus causing I to peak. This same statistical effect also explains the fine structure of the angular distribution in Figure 10.

These results clearly indicate that Lambert's law is in substantial error for both perfect and imperfect reflectors.* It must be pointed out that the results presented here do not take into account blockage of the incident light by the physical structure of the heat receiver; they assume a full paraboloidal reflector with no blockage. The inclusion of such blockage is expected to lead to further deviations from Lambert's law.

The gross errors of the Lambertian assumption means that plane focal surface results cannot be used to calculate cavity performance. The reflector cannot be isolated and independently optimized from the heat receiver; instead, both the reflector and the cavity must be studied as components of a proposed solar power system with the system being optimized from a systems viewpoint. In fact, it can be shown that the use of plane focal surface results in the prediction and optimization of solar power systems is completely redundant. To see this, let us consider a system consisting of a solar reflector and a heat receiver. Define

η_{system} = power out of the heat receiver/total power incident on the reflector

η_{cavity} = power out of the heat receiver/total power into heat receiver

$\eta_{collection}$ = power collected in area πr^2 /total power reflected by the reflector

Γ = coefficient of reflection of the reflector surface

Then

$$\eta_{system} = \Gamma \eta_{cavity} \eta_{collection}$$

In order to optimize this system we must maximize η_{system}.

*It is interesting to note that the cylindrical cavity results shown in Figures 11 and 12 indicate that the design of a solar power system on the basis of Lambert's law could lead to significant problems and/or failures. The shift in position and magnitude of the peak of I along the wall of the cylindrical cavity simply cannot be ignored.

Now, it is clear that $\eta_{collection}$ is easily obtained from plane focal surface results—independent of any internal cavity design. The determination of η_{cavity}, however, presents problems. The assumption that the cavity opening behaves as if it were a gray body would serve to determine η_{cavity} as a function only of the cavity opening—independent of the internal cavity design. Thus, the reflector design could be optimized independent of the internal cavity design. As we pointed out earlier, however, this assumption is incorrect, as will be seen later on in this paper; thus η_{cavity} must depend on the internal cavity design.

Furthermore, we have also shown that the use of plane focal surface results via Lambert's law to predict the incident energy flux on the cavity wall is incorrect. In other words we have shown that η_{cavity} cannot be determined from plane focal surface results; instead the correct energy flux incident on the cavity walls must be used. Thus, the only possible use left for plane focal surface results would be determine $\eta_{collection}$. Thus, however, is superfluous as once the energy flux incident on the walls of the cavity is known, it is a simple matter to integrate and calculate $\eta_{collection}$.

In general, the calculation of η_{cavity} is a complicated problem. It depends upon the cavity geometry, cavity opening, internal wall temperature distribution (as determined by the interface with the heat exchanger and/or thermal energy storage material), distribution of incident energy flux from the reflector, and the material properties of the cavity walls. Since the prediction of η_{cavity} depends upon reflector design and since $\eta_{collection}$ is easily obtained from the incident energy flux on the cavity wall without using plane focal surface results, it readily becomes apparent that in order to optimize η_{system}, we must study η_{cavity}. The calculation of $\eta_{collection}$ is a by-product of the calculation of η_{cavity}. Thus, the question of the design of an optimum reflector cannot be answered independent of the cavity through the use of plane focal surface results and $\eta_{collection}$. Instead, the system must be optimized from a systems viewpoint with emphasis being placed on the determination of η_{cavity}.

CAVITY ANALYSIS

Let us now consider the calculation of the performance of cylindrical heat receivers. The approach to be utilized can best be described as an "open cavity" Fredholm integral equation approach. Because of the availability of the generalized reflector model, no specific directional distribution for the incident radiation will be utilized in this approach; instead, the actual energy flux incident on the wall of the cavity will be used.

Consider the sketch shown in Figure 14. Define

x = a coordinate specifying a point on the cylindrical cavity

$f(x)$ = incident energy flux on the wall of the cavity

$T(x)$ = assumed temperature distribution of the wall of the cavity

σ = Stefan-Boltzmann constant

ϵ = emissivity of the cavity wall

α = absorptivity of the cavity wall

$K(x,x')$ = kernel of the integral equation. This is a geometrical factor that describes the cavity geometry. It is an infinitesimal area view factor.

$\nu(x)$ = total energy flux reflected and emitted from the point x of the cavity

Assuming that the walls of the cavity are diffuse*, one obtains

$$\nu(x) = \epsilon\sigma T^4(x) + (1-\alpha)\left[f(x) + \int_{\substack{\text{walls}\\ \text{of the}\\ \text{cavity}}} K(x,x')\,\nu(x')dx' \right].$$

*It is important to emphasize that the material walls of the cavity are assumed to emit and reflect radiation diffusely. Specular reflection has been neglected because the precise techniques of analysis have never been worked out. Crude techniques of analysis do exist (19); however, accurate techniques that take into account the finite size of the solar source do not presently exist.

Here the integral extends over only the material walls of the cavity—hence, the designation "open cavity" approach. The calculation of the kernel $K(x,x')$ for the cylindrical geometry is straightforward and will not be discussed here. The numerical solution of this Fredholm integral equation is carried out by using the well known Liouville-Neumann series. A temperature distribution $T(x)$ is assumed and this equation is then solved for $\nu(x)$. When $\nu(x)$ is known, the performance of the cavity can then be calculated.

Some initial results have been obtained for a 60° paraboloidal reflector ($R = 1.0$) coupled to a cylindrical cavity with $R_c = .03$ and $\ell/d = 2$. The cavity opening was arbitrarily chosen so that $\eta_{collection} = .90$.

Define

A = area of cavity opening

Q_R = total energy reradiated out of the cavity opening

η_{cavity} = efficiency of the cavity = total energy conducted through the walls of the cavity/total energy entering the cavity.

Figure 15 shows the results obtained for this cavity when it is assumed to be isothermal at $1000^{\circ}K$, $1400^{\circ}K$, $1800^{\circ}K$ for an imperfect 60° paraboloidal reflector with $\sigma_x = 5'$, $\sigma_y = 10'$. Figure 16 shows the same results obtained for an isothermal $1400^{\circ}K$ cavity with a perfect ($\sigma_x = \sigma_y = 0$) 60° paraboloidal reflector. In both cases the correct energy flux incident on the cavity walls was used (as given in Figures 12 and 11, respectively).

These results differ significantly from the usual engineering approach used in the design of solar power systems—namely that the cavity opening can be treated as if it were a gray body ($Q_R / A\sigma T^4 < 1$)*. Those who use this gray cavity approach argue that if the cavity opening were small, the cavity opening would behave like a black body. Hence, as the opening is made larger, the cavity opening ought to behave like a gray body. They have, however, neglected the important fact that this cavity is fundamentally different as it is driven by energy entering through the opening instead of through the walls. The results presented here offer perhaps the first

---

Specifically, in the design of solar power systems it is usually assumed that the cavity losses can be separated into losses due to multiple reflections (these are often neglected) and losses due to reradiation effects from a gray cavity (calculated as if the cavity opening were a gray body). Losses from multiple reflections, if included, are treated as corrections to gray cavity results. From the basic integral equation it is clear that this decomposition into reflected and reradiated losses has no meaning—only the total has a physical meaning. Hence, it is meaningless to treat multiple diffuse reflection losses as a correction to gray cavity reradiation losses.

realistic estimates of cavity performance for a cavity coupled to a solar reflector. They clearly show the importance of the absorptivity of the material surface of the cavity walls and point out that a gray cavity assumption is erroneous.

The results and experience that have been obtained clearly show that the cavity is a major design problem; a very detailed cavity analysis must always be made in order to estimate cavity performance accurately.* Furthermore, since the incident flux distribution on the cavity wall is a function of the actual reflector used and since the cavity wall temperature distribution is a function of whatever connects to the cavity walls (thermal energy storage material, heat exchanger, etc.), the cavity cannot be studied and optimized independently. Instead, a systems approach must be utilized.

The importance of and need for performing extensive detailed systems studies of solar-thermal energy conversion systems cannot be overemphasized. Efforts to date have only begun to "scratch the surface"— thermal energy storage materials must be included, various cavity geometries must be studied, other types of heat exchangers and direct conversion devices must be used, etc.

---

* It is important to point out here the work of Al Lowi and associates at Aerospace Corp. (16, 17,18). They are performing the most extensive and realistic solar-thermal energy space power systems study to date. Their system presently consists of a solar reflector, cylindrical cavity, and a gaseous heat exchanger. They are using the optical analysis techniques previously discussed to calculate the energy flux on the walls of the cavity. Their cavity analysis technique is basically similar to that described in this paper, except they use a finite difference approach to the problem (16). Thus, they use finite area view factors and invert a matrix to solve the cavity problem. In addition, they also take into account spectral properties of the cavity walls by using spectral decompositions of the radiation. For the heat exchanger analysis they use a thermal analyzer network solution (17). In order to solve for the cavity wall temperature distribution they perform an iteration between the cavity and heat exchanger routines. Their results (restricted to isothermal walls) agree with those we obtain by solving the Fredholm integral equation.

CONCLUSIONS

A mathematical model for analysis of actual solar collectors has been developed. This solar collector model is truly a mathematical solar simulator; thus it is a necessary and indispensable tool in any realistic systems study involving a solar collector. Because of the broad scope and generality of this model, its perfection now provides the solar-thermal energy space power system designer with tools that have been heretofore unavailable.

This mathematical solar simulator was used to investigate the interface between the collector and the heat receiver—the cavity opening. The assumption of Lambert's law to describe the directional characteristics of this interface was shown to be in substantial error.

In the design of a solar-thermal energy space power system, the total system efficiency—not the individual component efficiencies —must be optimized. In the calculation of system efficiency, it was shown that the calculation of cavity efficiency is more basic than the calculation of collection efficiency as the latter is a by-product of the calculation of the former.

An "open cavity" Fredholm integral equation approach and the valid directional distribution were utilized to calculate the performance of some typical isothermal cylindrical cavities. The results presented clearly show that the usual engineering "gray cavity opening" approach is incorrect. The design of cavities for use with solar reflectors is still a very difficult problem area with much work remaining to be done.

Proper use of existing analytical capabilities for the accurate mathematical simulation of solar-thermal energy space power systems can greatly expidite the development of solar power systems.

REFERENCES

1. Cabannes, F. and Le Phat Vinh, A. "Calcul De La Répartition De L'énergie Solaire Réfléchie Par Un Miroir Parabolique, "Le Journal De Physique Et Le Radium, 15 (December 1954) p 817.

2. Hukuo, N. and Mii, H. "Design Problems of a Solar Furnace, "Solar Energy, 1, No. 203 (1957) pp 108-114.

3. McClellan, D. H. and Stephens, C. W. "Solar-Thermal Energy Sources," Vol. II, Energy Conversion Systems Reference Handbook, WADD TR 60-699 (September 1960).

4. Technical Proposal for Solar Energy Thermionic Conversion System for Mars Probe, Allison Division G.M.C., EDR 2011 (10 March 1961).

5. Löf, G.O.G. and Duffie, J.A. "Optimization of Focusing Solar-Collector Design," Journal of Engineering for Power (July 1963) pp 221-228.

6. Liu, B.Y.H. and Jordan, R.C. Performance and Evaluation of Concentrating Solar Collectors for Power Generation, ASME Paper No. 63-WA-114.

7. Silvern, D.H. An Analysis of Mirror Accuracy Requirements for Solar Power Plants, Am. Rocket Society Paper 1179-60.

8. Fuller, F. E. Mathematical Model of Factors Affecting Solar Energy Collection Efficiency, WADD TR 60-907, Air Force Contract AF33(616)-7316 (30 December 1960).

9. Kerr, D. Private oral communication with General Electric (6 November 1963).

10. Dresser, D. L., Hietbrink, E. H., McClure, R.B., Whitaker, R.O. Allison Research and Development of Solar Reflectors, Allison Division G.M.C., EDR 1826 (15 August 1960).

11. Schrenk, G. Theoretical Analysis of the Optics of Fresnel Mirrors, Allison Division G.M.C., APS Report No. 54 (16 May 1961).

12. Schrenk, G. Analysis of Actual Mirrors, Allison Divison G.M.C., APS Report No. 55 (26 June 1961).

13. Schrenk, G. Theoretical Analysis of Solar Reflectors, Allison Division G.M.C., EDR 3193 (1 July 1963).

14. Schrenk, G. IBM 7090 Computer Program for Analysis of Solar Reflectors (Deck D70E), Allison Division G.M.C., EDR 3666 (8 February 1963). Schrenk, G. IBM 7090 Computer Program for Design of Spherical Fresnel Reflectors (Deck D70S), Allison Division G.M.C., EDR 3664 (1 Feb. 1963). Schrenk, G. IBM 7090 Computer Program for Summation of Fresnel Reflector Results (Deck D70Z), Allison Division G.M.C., EDR 3665 (4 February 1963).

15. Schrenk, G. Final Report—Analysis of Solar Reflectors—Mathematical Theory and Methodology for Simulation of Real Reflectors, Air Force Contract AF04(695)-335, Allison Division G.M.C., EDR 3693 (16 December 1963).

16. Lowi, A. Radiation Transfer Theory and Methodology for Design of Cavity Type Solar Absorbers, Dept. of Engineering Report (unpublished), U. of California (10 January 1962).

17. Wright, C.C. Development of a Computer Program Subroutine for the Cavity-Absorber Heat Exchanger, Aerospace Corp. Report A62-1765.36-5 (3 December 1962).

18. Ames, B. and Sallin, E. Solar Thermal Energy Conversion Study Production Manual, Aerospace Program Manual PH 015 A.

19. Sparrow, E.M. Radiant Absorption Characteristics of Concave Cylindrical Surfaces, ASME Paper No. 61—WA-145.

FIGURE CAPTIONS

Figure 1. Definition of terms for a typical paraboloidal solar collector.

Figure 2. Rim angle effects for a paraboloidal reflector with $\sigma_x = \sigma_y = 0$, $\beta = 0$.

Figure 3. Orientation effects for a 60° paraboloidal reflector with $\sigma_x = \sigma_y = 0$.

Figure 4. Surface error effects for a 60° paraboloidal reflector with $\sigma_x = 0$, $\sigma_y \neq 0$, $\beta = 0$.

Figure 5. Surface error effects for a 60° paraboloidal reflector with $\sigma_x \neq 0$, $\sigma_y = 0$, $\beta = 0$.

Figure 6. Surface error effects for a 60° paraboloidal reflector with $\sigma_x = \sigma_y \neq 0$, $\beta = 0$.

Figure 7. Surface error effects for a 60° paraboloidal reflector with $\sigma_x = 5'$, $\sigma_y = 10'$, $\beta = 0$ and $\sigma_x = 10'$, $\sigma_y = 5'$, $\beta = 0$.

Figure 8. Definition of terms for the cavity configurations studied.

Figure 9. Directional distribution as determined from the hemispherical cavity of Figure 8 for a 60° paraboloidal reflector with $\sigma_x = \sigma_y = 0$.

Figure 10. Directional distribution as determined from the hemispherical cavity of Figure 8 for a 60° paraboloidal reflector with $\sigma_x = 5'$, $\sigma_y = 10'$.

Figure 11. Incident energy flux on the walls of a typical cylindrical cavity for a 60° paraboloidal reflector with $\sigma_x = \sigma_y = 0$.

Figure 12. Incident energy flux on the walls of a typical cylindrical cavity for a 60° paraboloidal reflector with $\sigma_x = 5'$, $\sigma_y = 10'$.

Figure 13. Histogram to explain the peaking of I on the back wall of the cylinder as $x \to 0$ in Figure 12.

Figure 14. Definition of terms used in the cavity analysis.

Figure 15. Cylindrical isothermal cavity performance. 60° paraboloidal reflector with $\sigma_x = 5'$, $\sigma_y = 10'$, $\beta = 0$.

Figure 16. Cylindrical isothermal cavity performance. 60° paraboloidal reflector with $\sigma_x = \sigma_y = 0$, $\beta = 0$.

TYPICAL SOLAR COLLECTOR

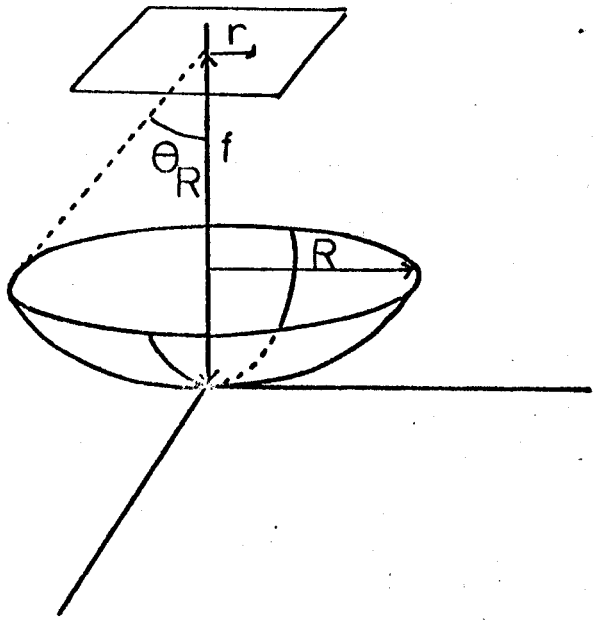

Figure 1

PARABOLOIDAL REFLECTORS

$R = 1.0$

$\sigma_x = 0$

$\sigma_y = 0$

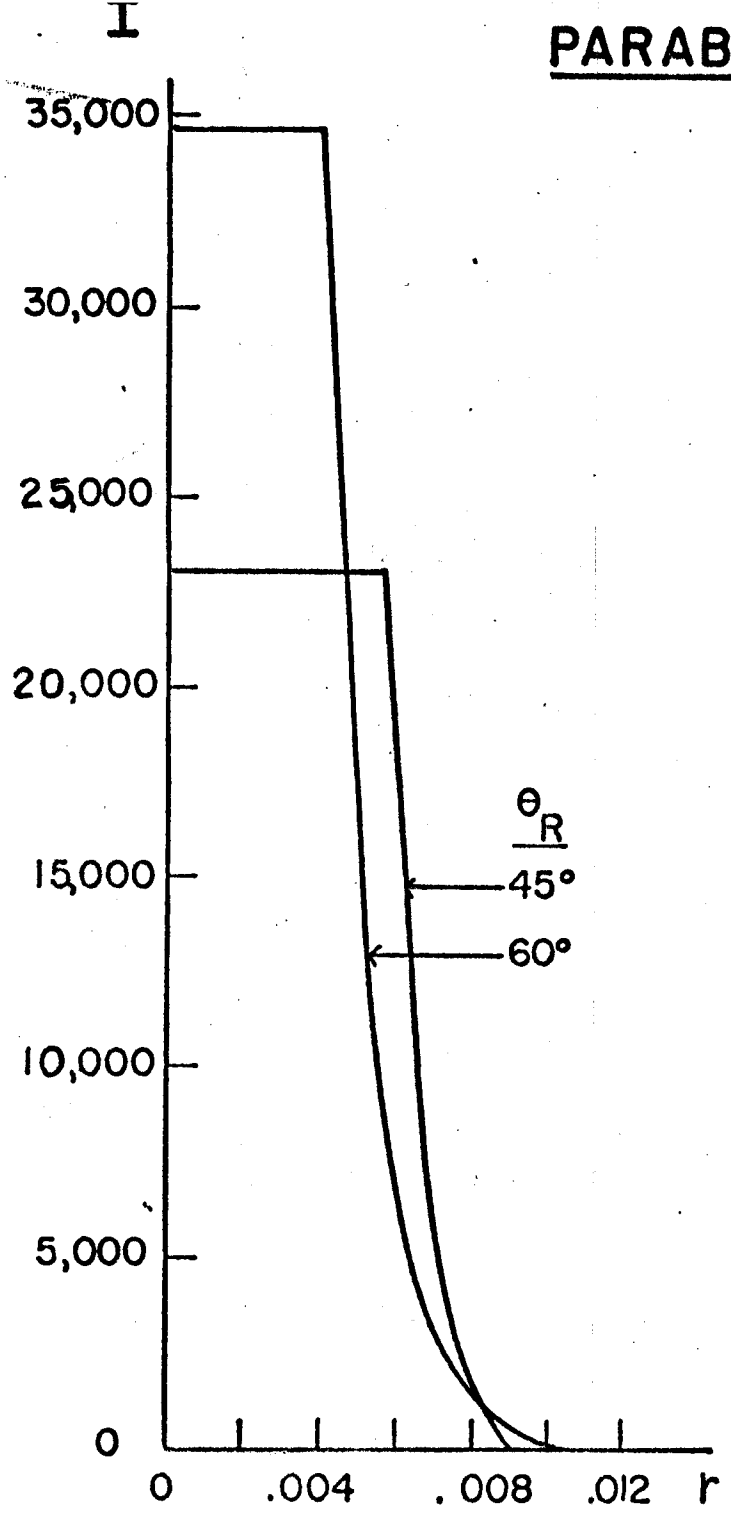

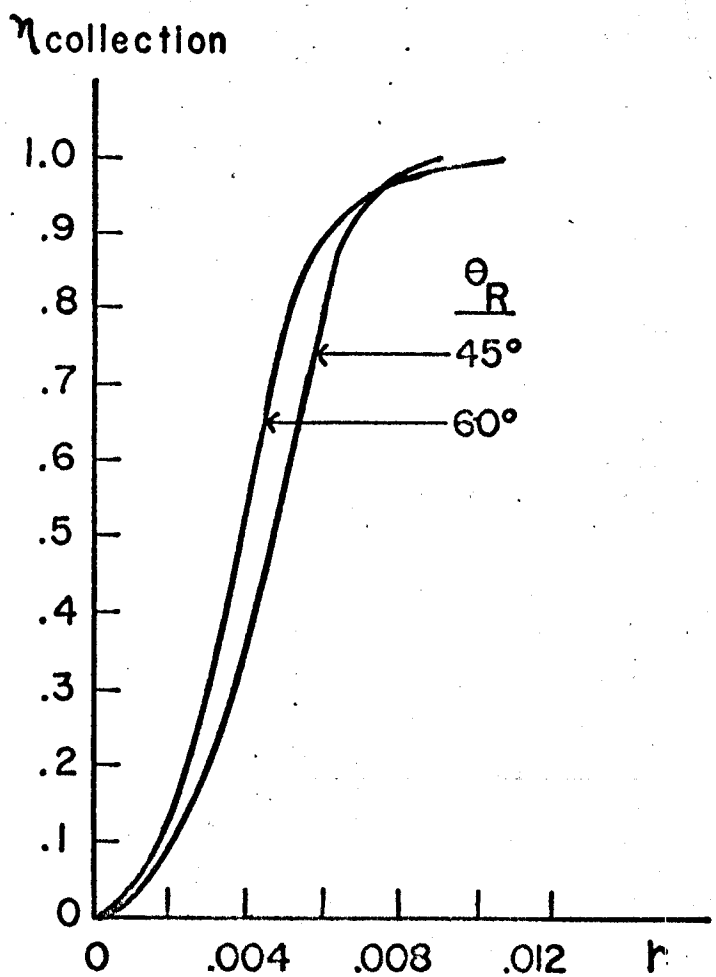

Figure 2

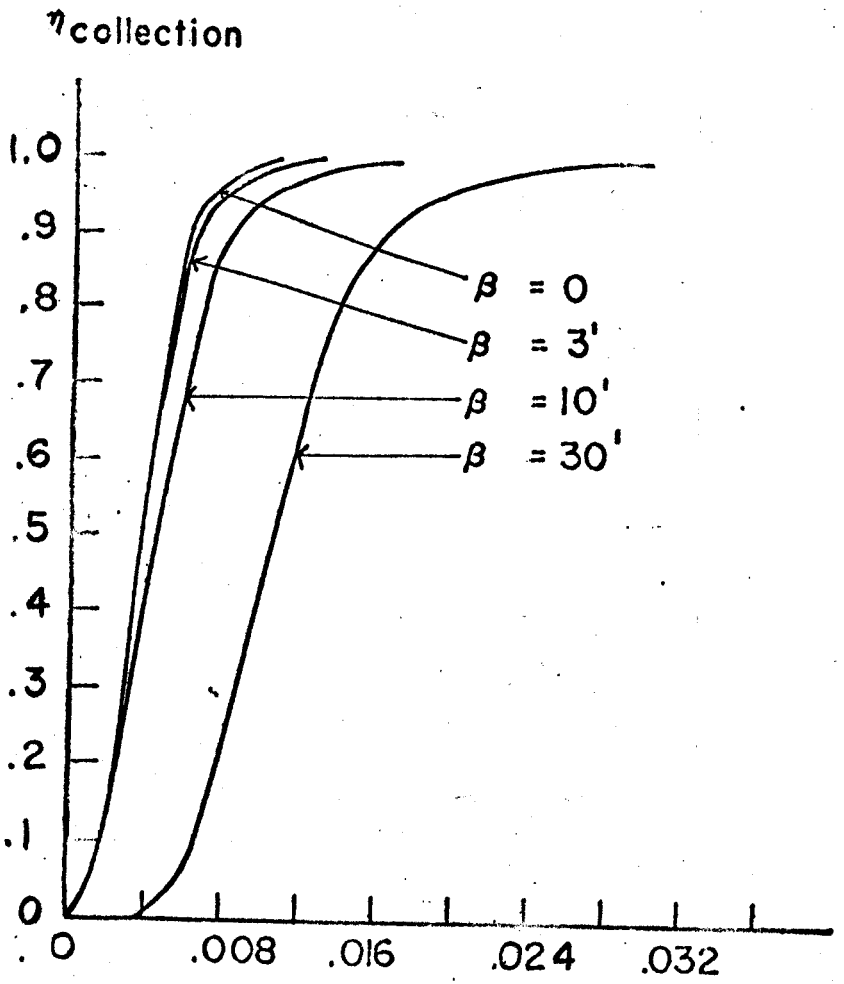

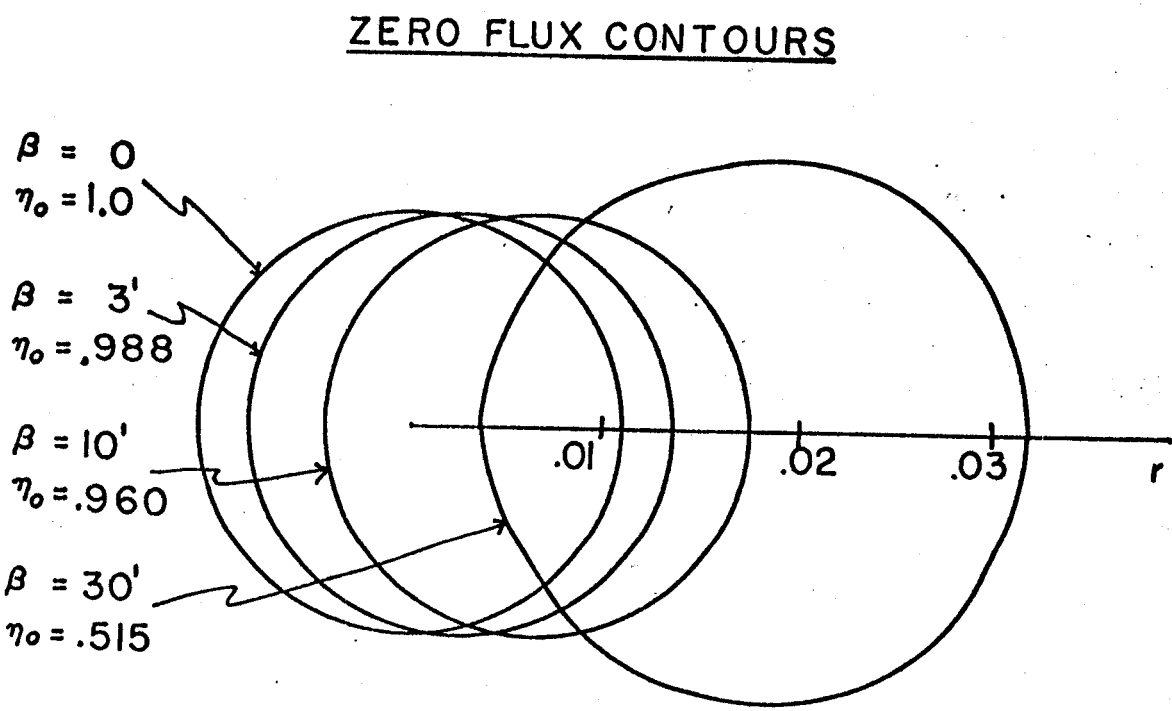

60° PARABOLOIDAL REFLECTOR

R = 1.0
σ_x = 0
σ_y = 0

Figure 3

60° PARABOLOIDAL REFLECTOR

R = 1.0

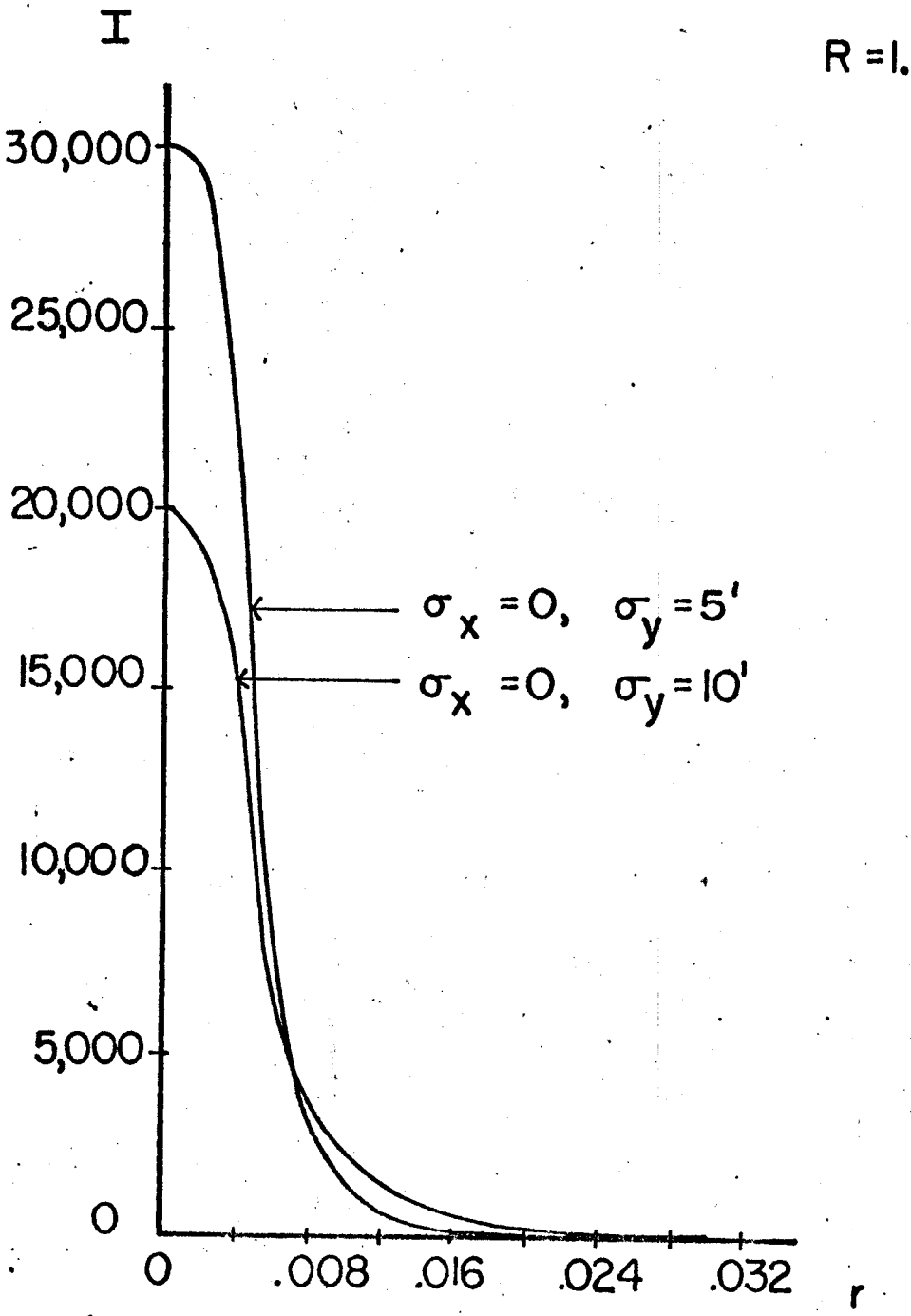

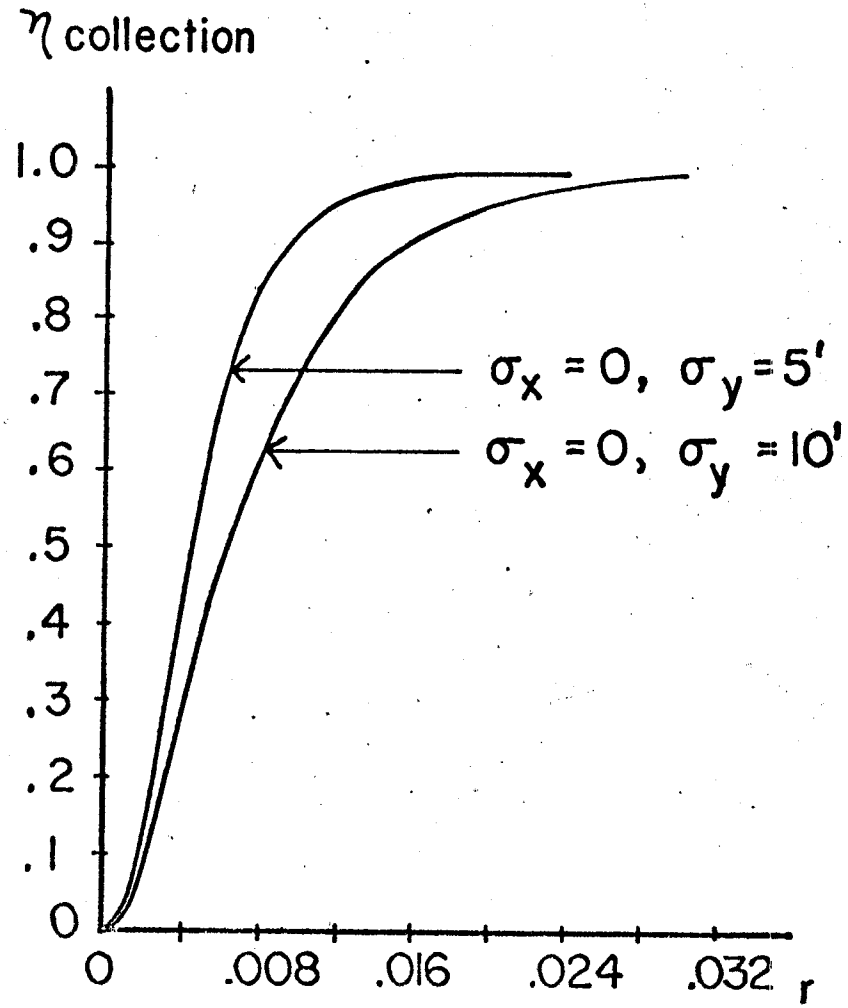

Figure 4

60° PARABOLOIDAL REFLECTOR

R = 1.0

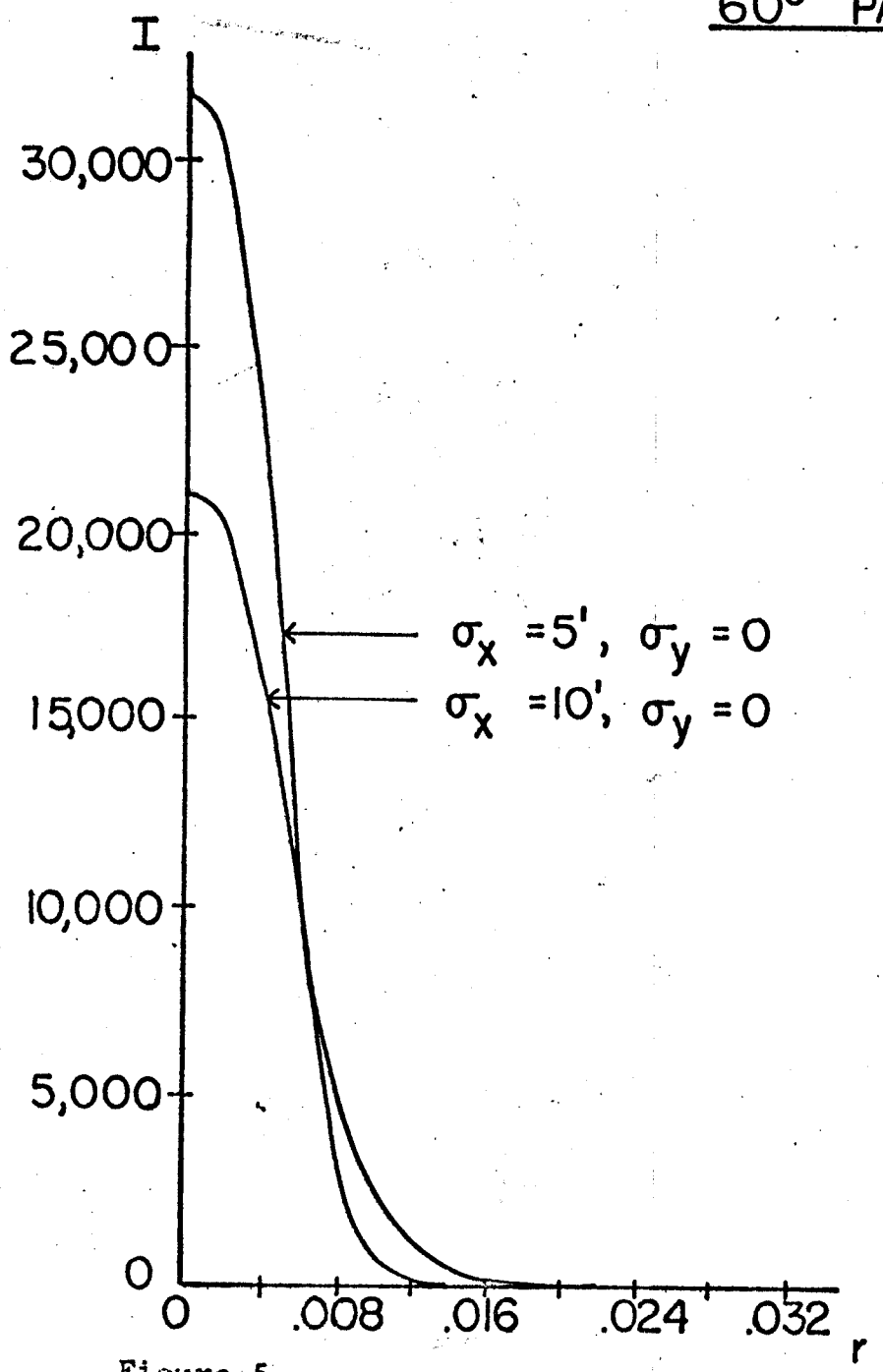

Figure 5

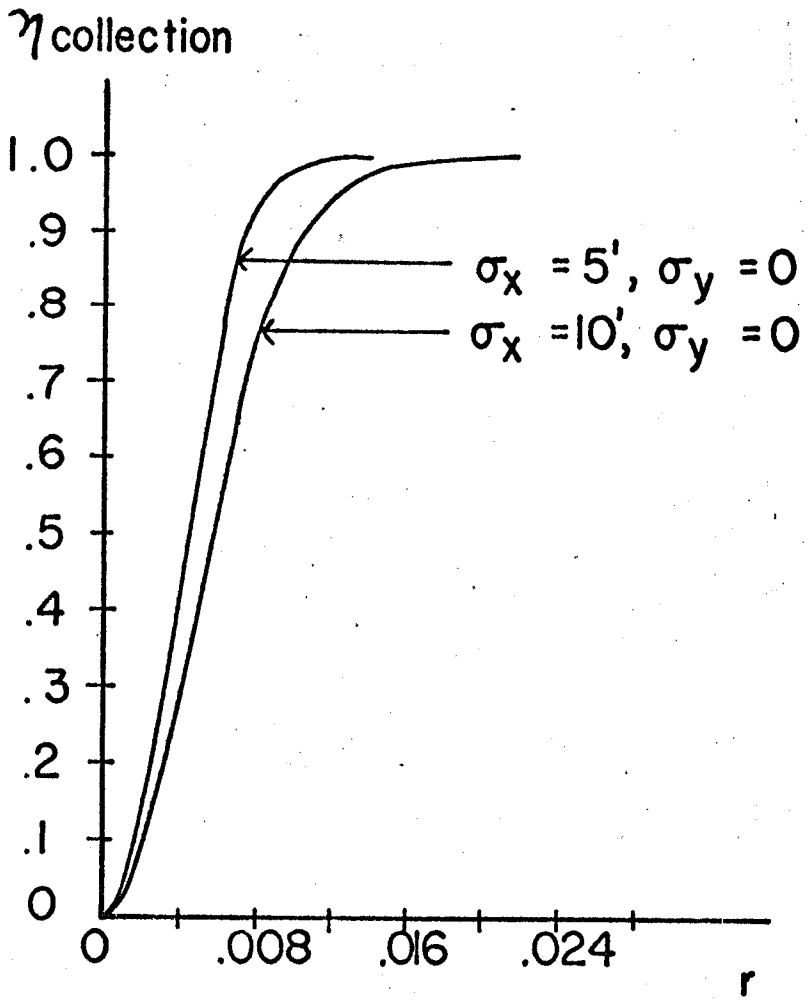

60° PARABOLOIDAL REFLECTOR

R = 1.0

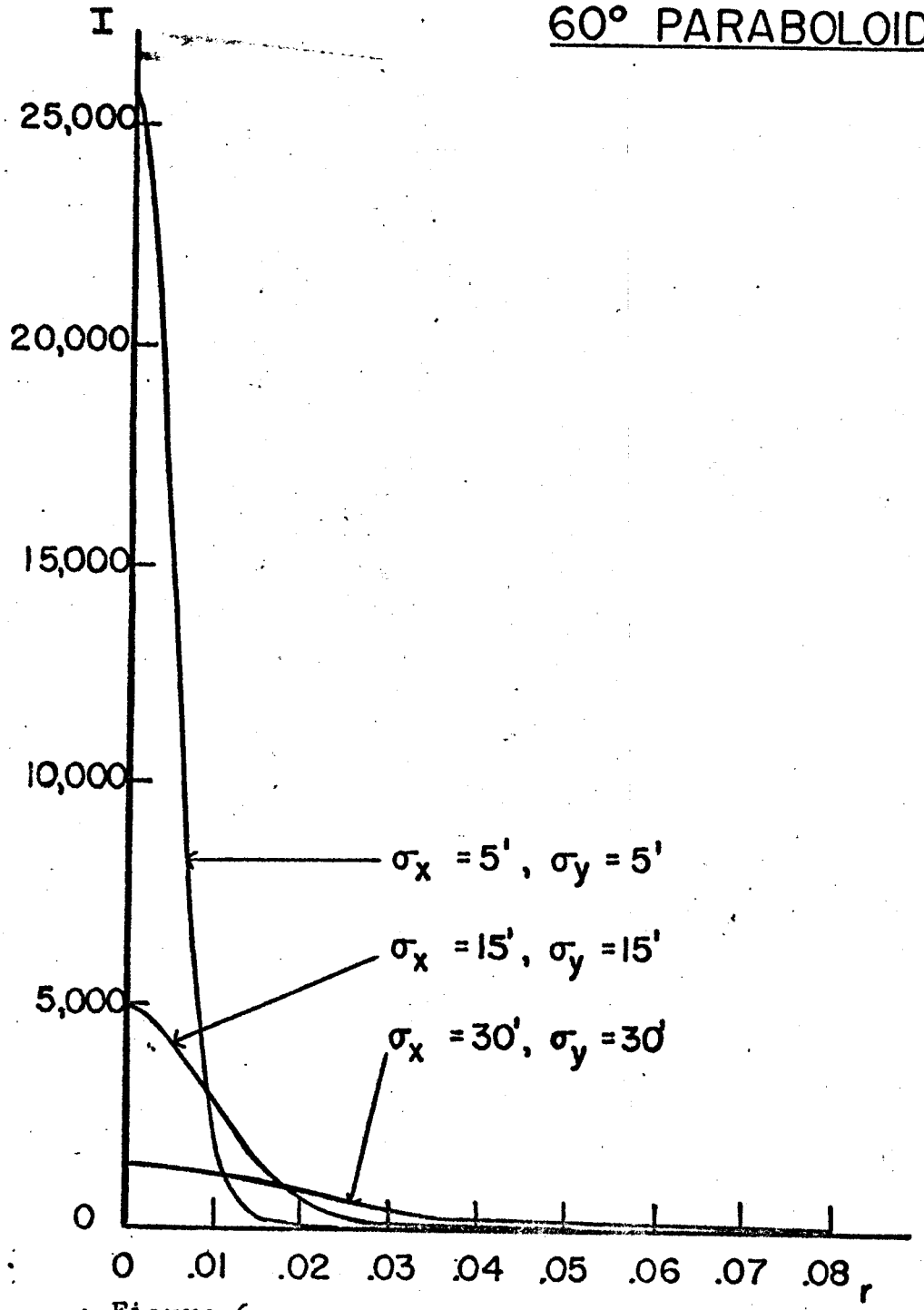

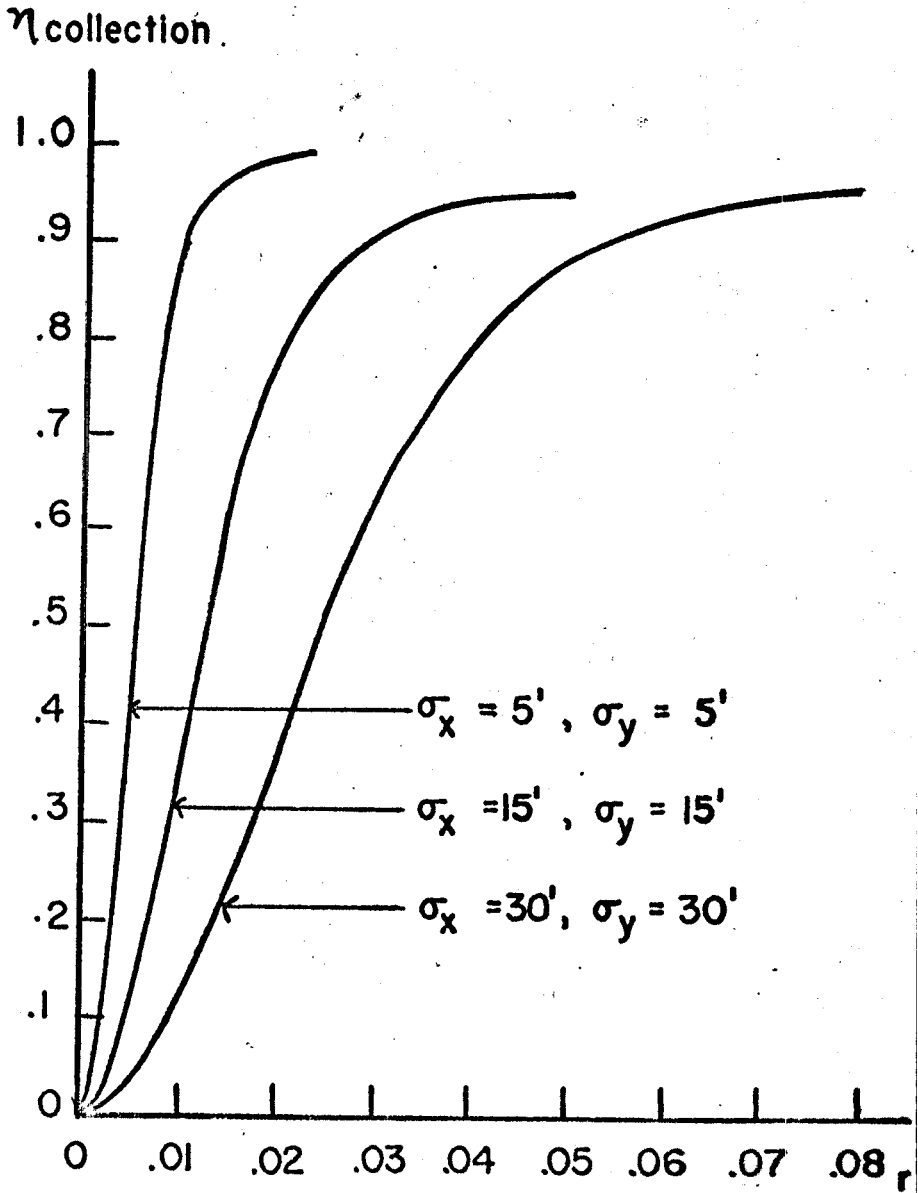

Figure 6

60° PARABOLOIDAL REFLECTORS

R = 1.0

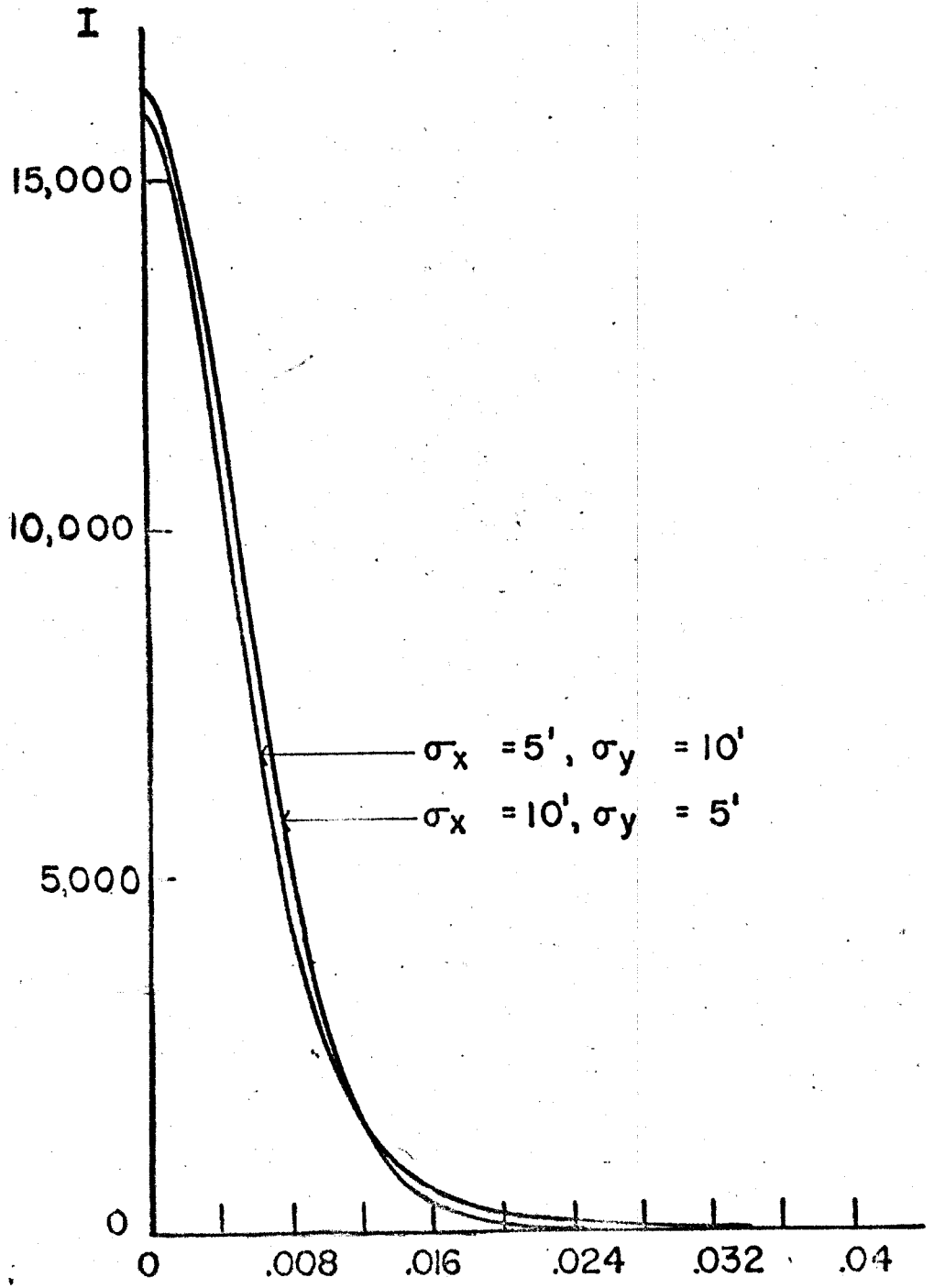

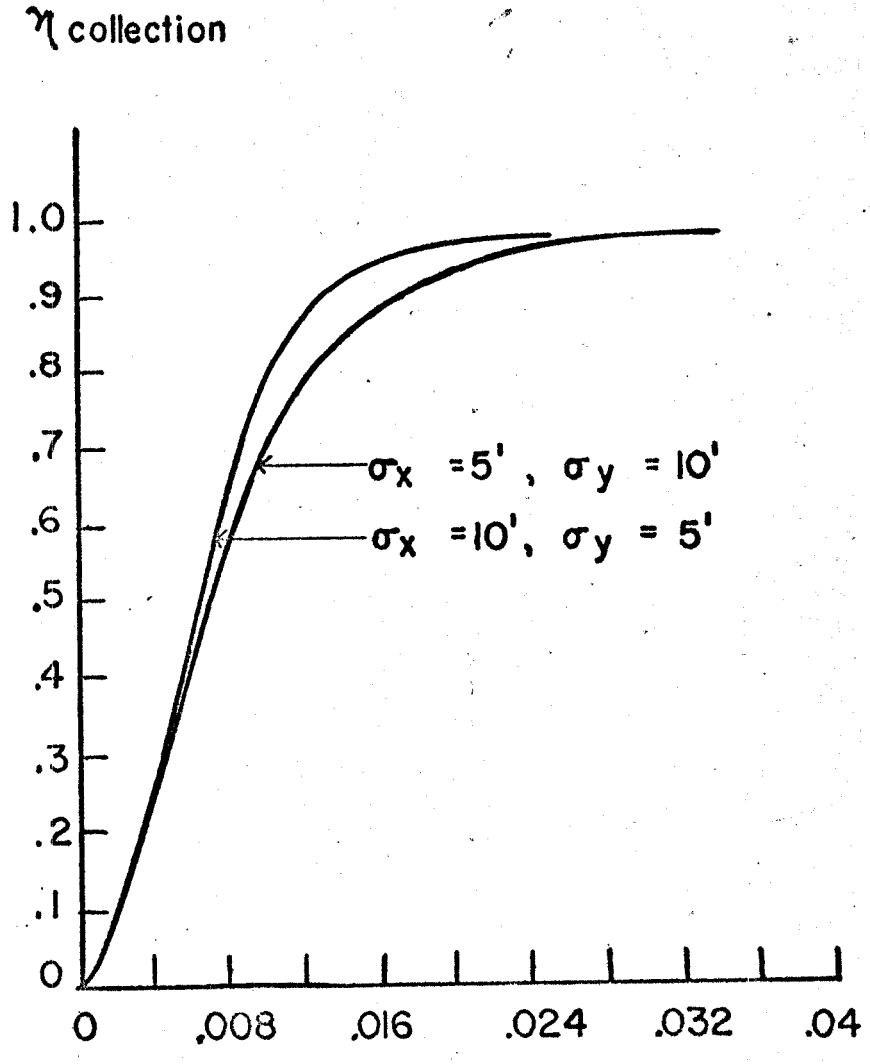

Figure 7

HEMISPHERICAL CAVITY

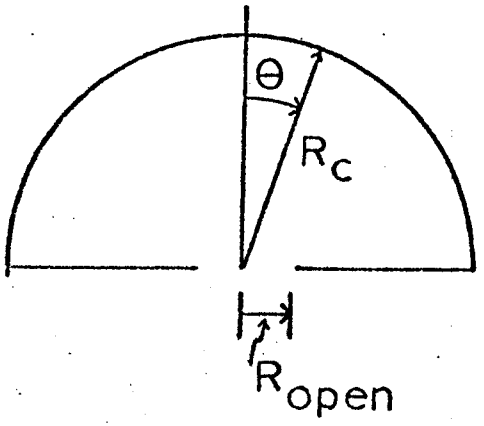

CYLINDRICAL CAVITY

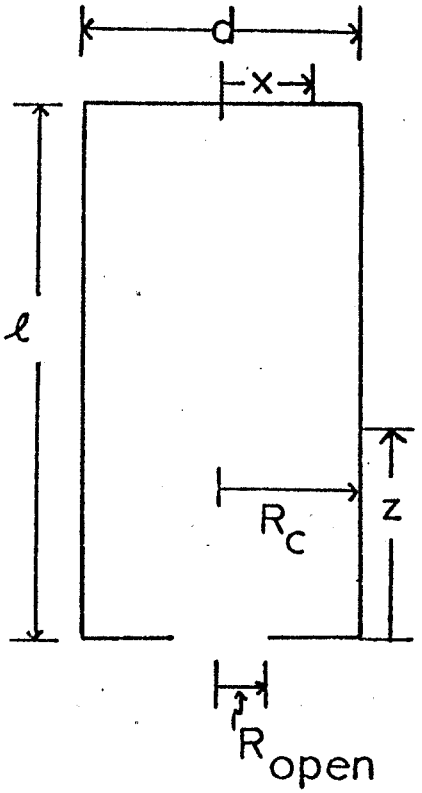

Figure 8

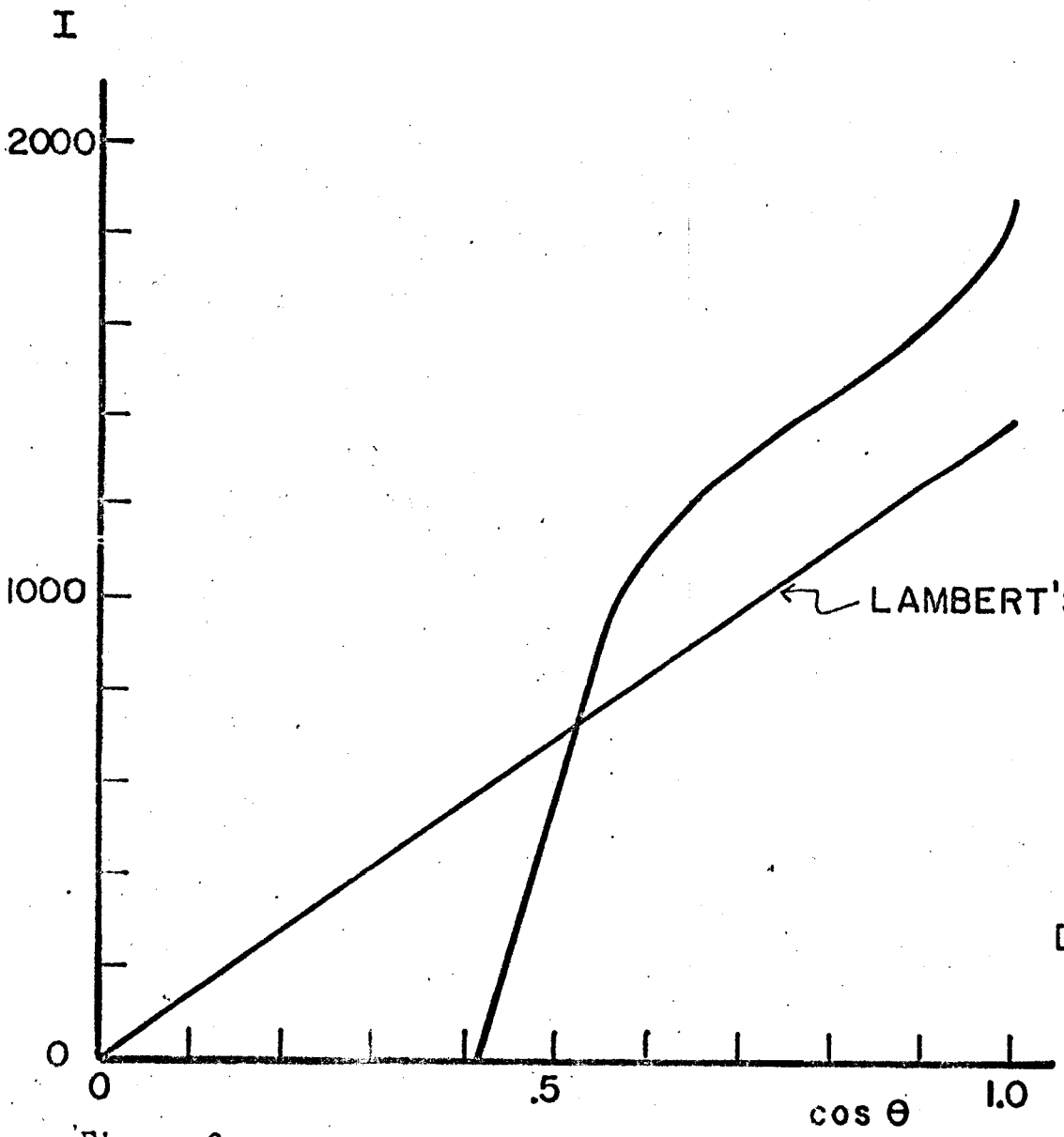

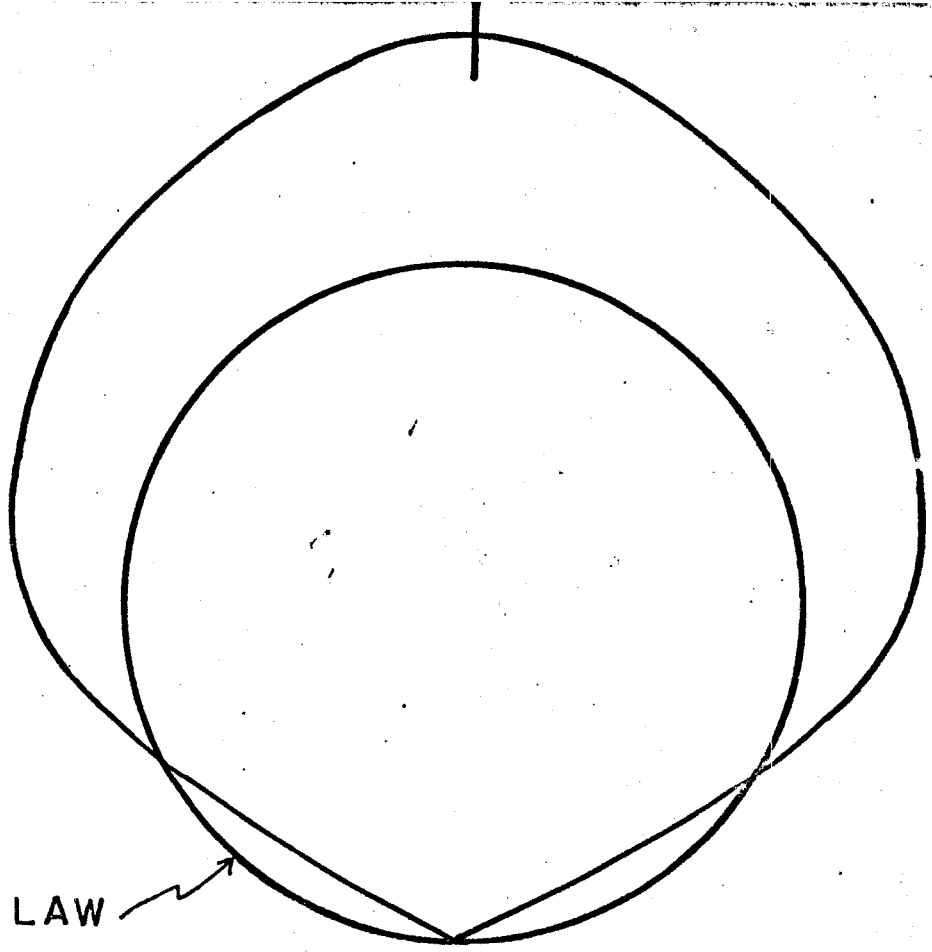

Figure 9

60° PARABOLOIDAL REFLECTOR

$R = 1.0$

$\sigma_x = 0$

$\sigma_y = 0$

DIRECTIONAL DISTRIBUTION DETERMINED FROM A HEMISPHERICAL CAVITY

$R_c = .02$

$R_{open} = .004$

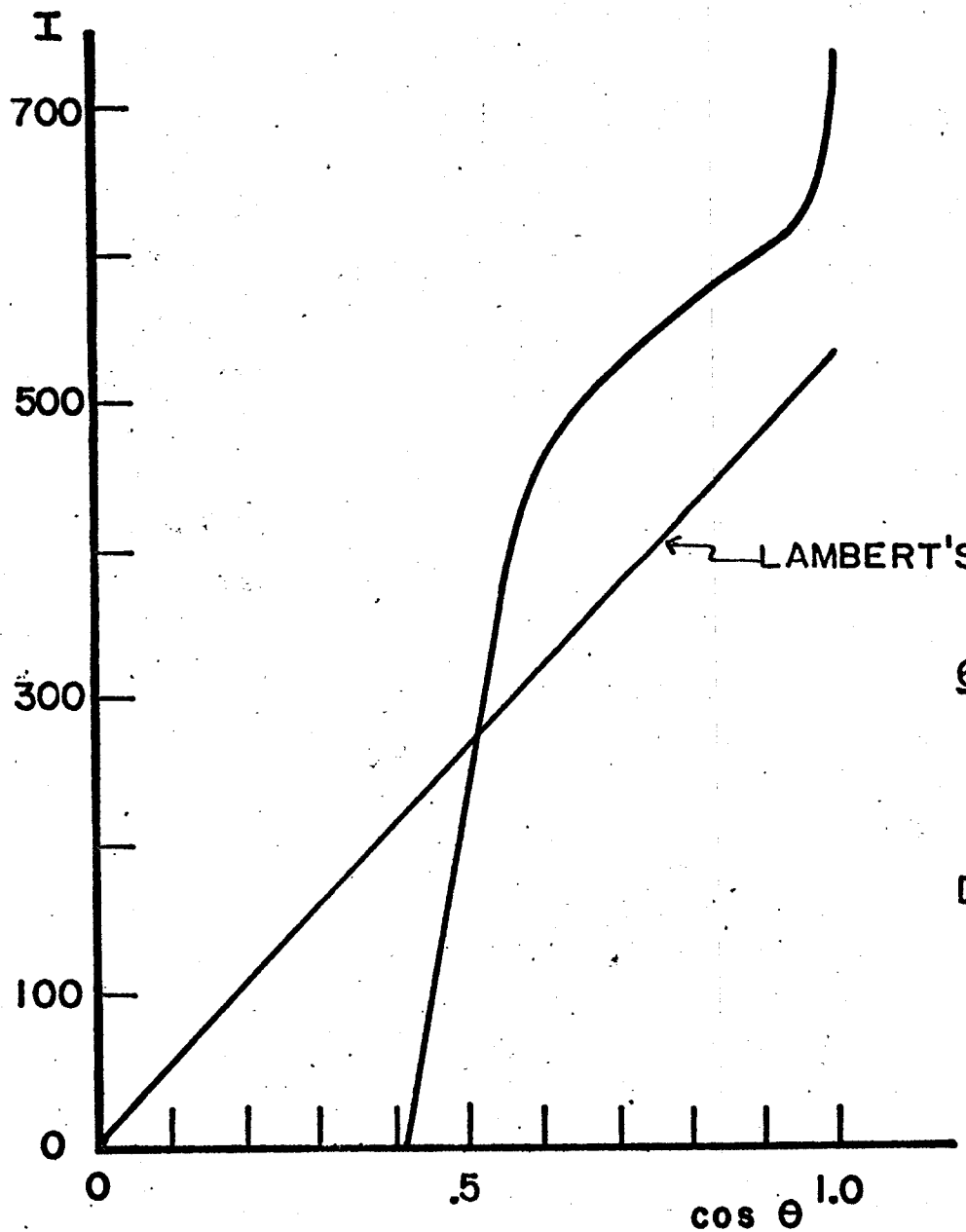

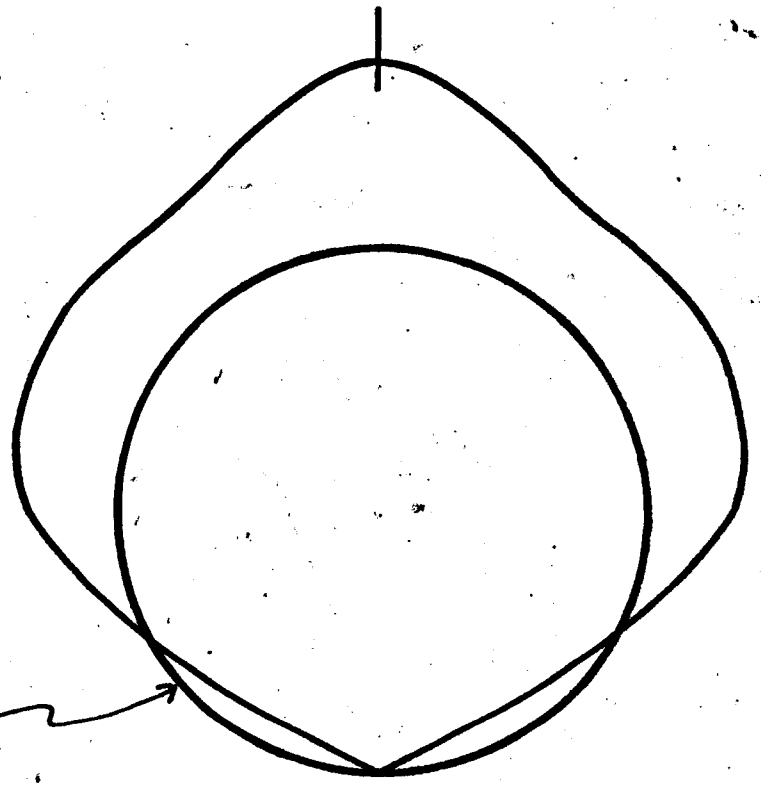

60° PARABOLOIDAL REFLECTOR

$R = 1.0$

$\sigma_x = 5'$

$\sigma_y = 10'$

DIRECTIONAL DISTRIBUTION DETERMINED FROM A HEMISPHERICAL CAVITY

$R_c = .02$

$R_{open} = .004$

Figure 10

I

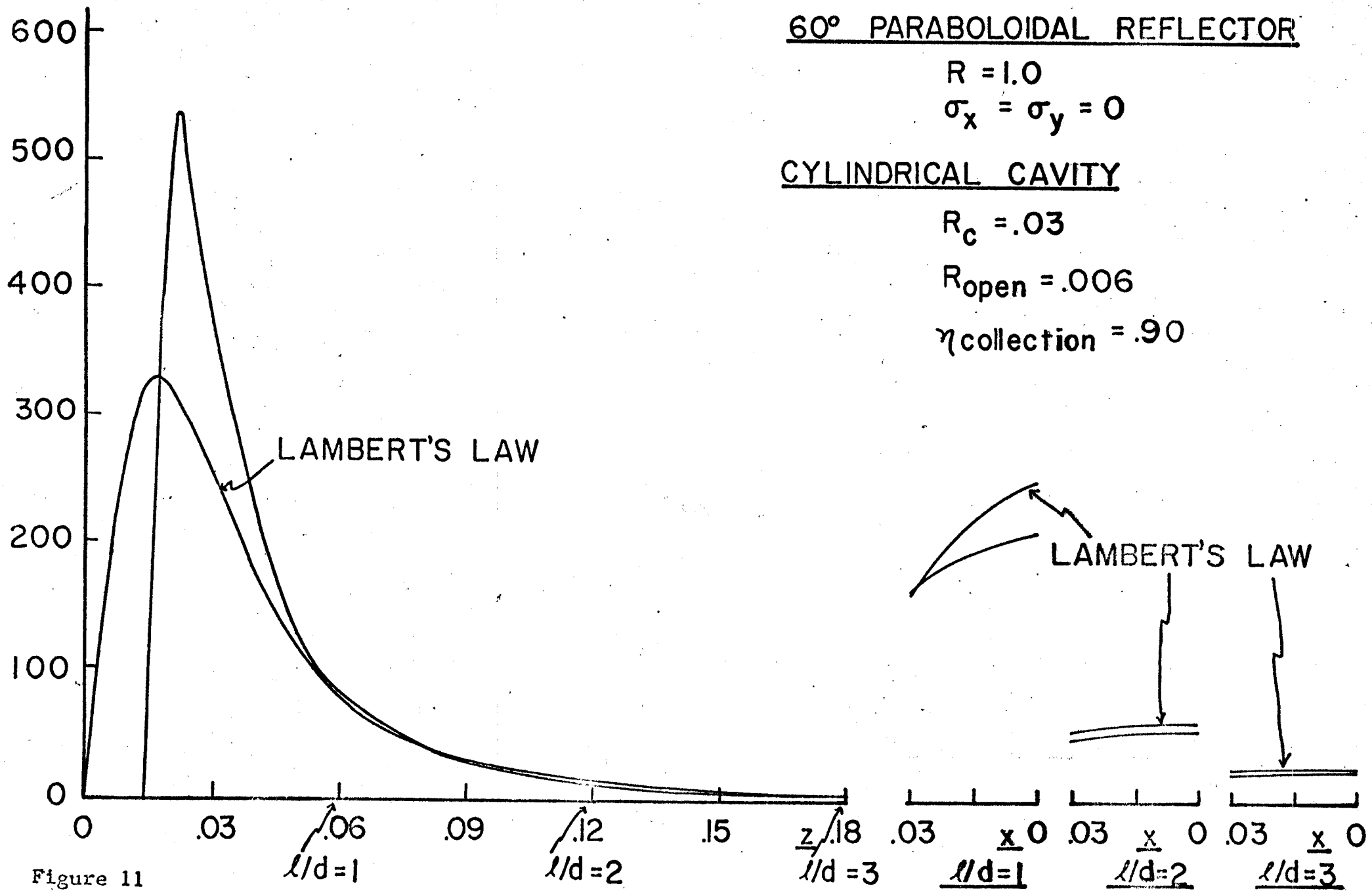
60° PARABOLOIDAL REFLECTOR
R = 1.0
$\sigma_x = \sigma_y = 0$
CYLINDRICAL CAVITY
R_c = .03
R_{open} = .006
$\eta_{collection}$ = .90
600
500
400
300
200
100
0
LAMBERT'S LAW
0
.03
.06
.09
.12
.15
z .18
ℓ/d = 1
ℓ/d = 2
ℓ/d = 3
LAMBERT'S LAW
.03
x 0
ℓ/d = 1
.03
x 0
ℓ/d = 2
.03
x 0
ℓ/d = 3

Figure 11

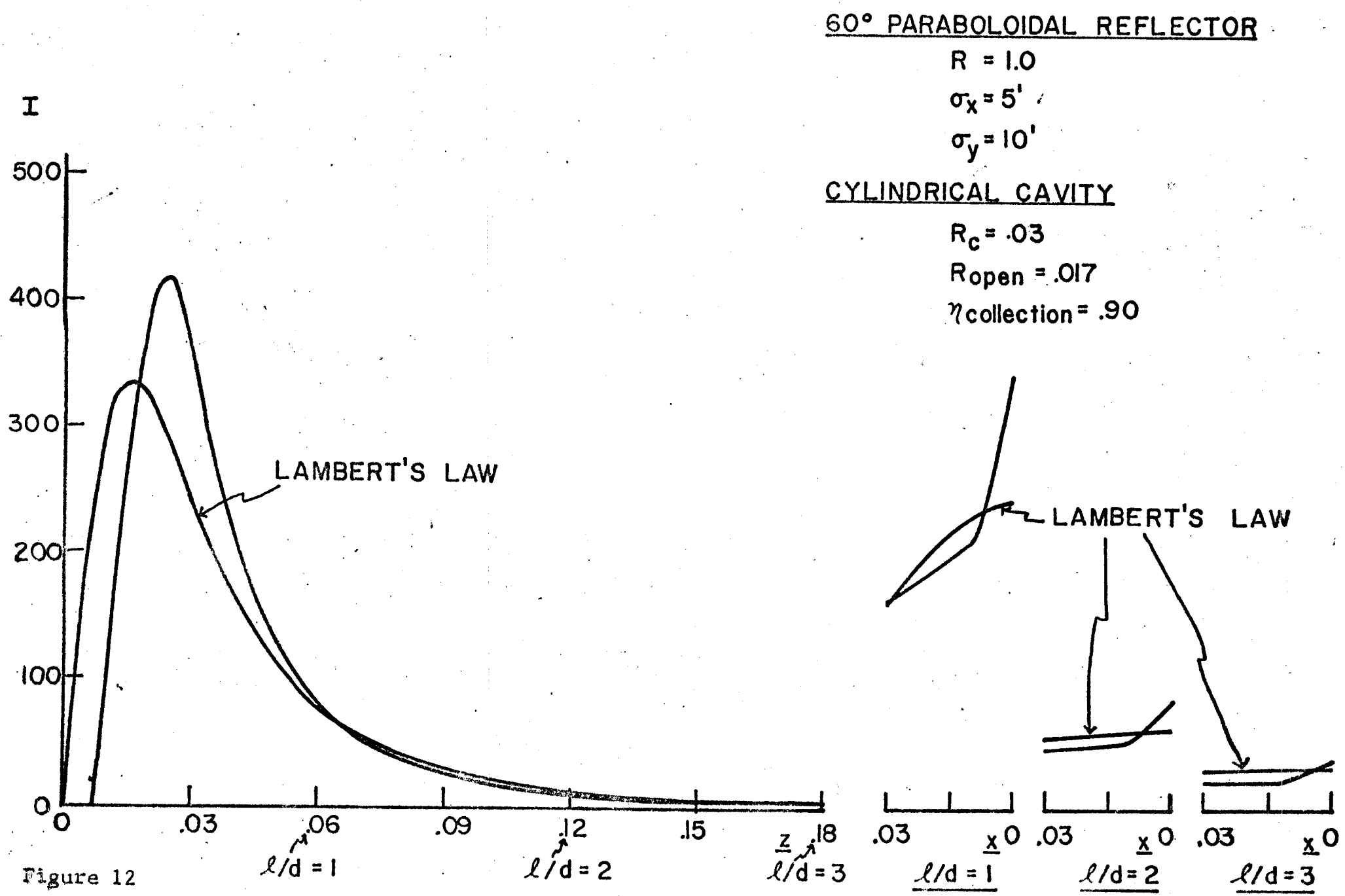
60° PARABOLOIDAL REFLECTOR
R = 1.0
σx = 5'
σy = 10'
CYLINDRICAL CAVITY
Rc = .03
Ropen = .017
ηcollection = .90
I
500
400
300
200
100
0
LAMBERT'S LAW
0
.03
.06
.09
.12
.15
.18
z
ℓ/d = 1
ℓ/d = 2
ℓ/d = 3
LAMBERT'S LAW
.03
x
0
ℓ/d = 1
ℓ/d = 2
ℓ/d = 3

Figure 12

HISTOGRAM OF NUMBER OF REFLECTOR AREAS VERSUS PROBABILITY

60° PARABOLOIDAL REFLECTOR

$R = 1.0$, $\sigma_x = 5'$, $\sigma_y = 10'$

Reflector is divided into 7500 equal areas

CYLINDRICAL CAVITY

$R_c = .03$, $R_{open} = .017$, $\eta_{collection} = .90$

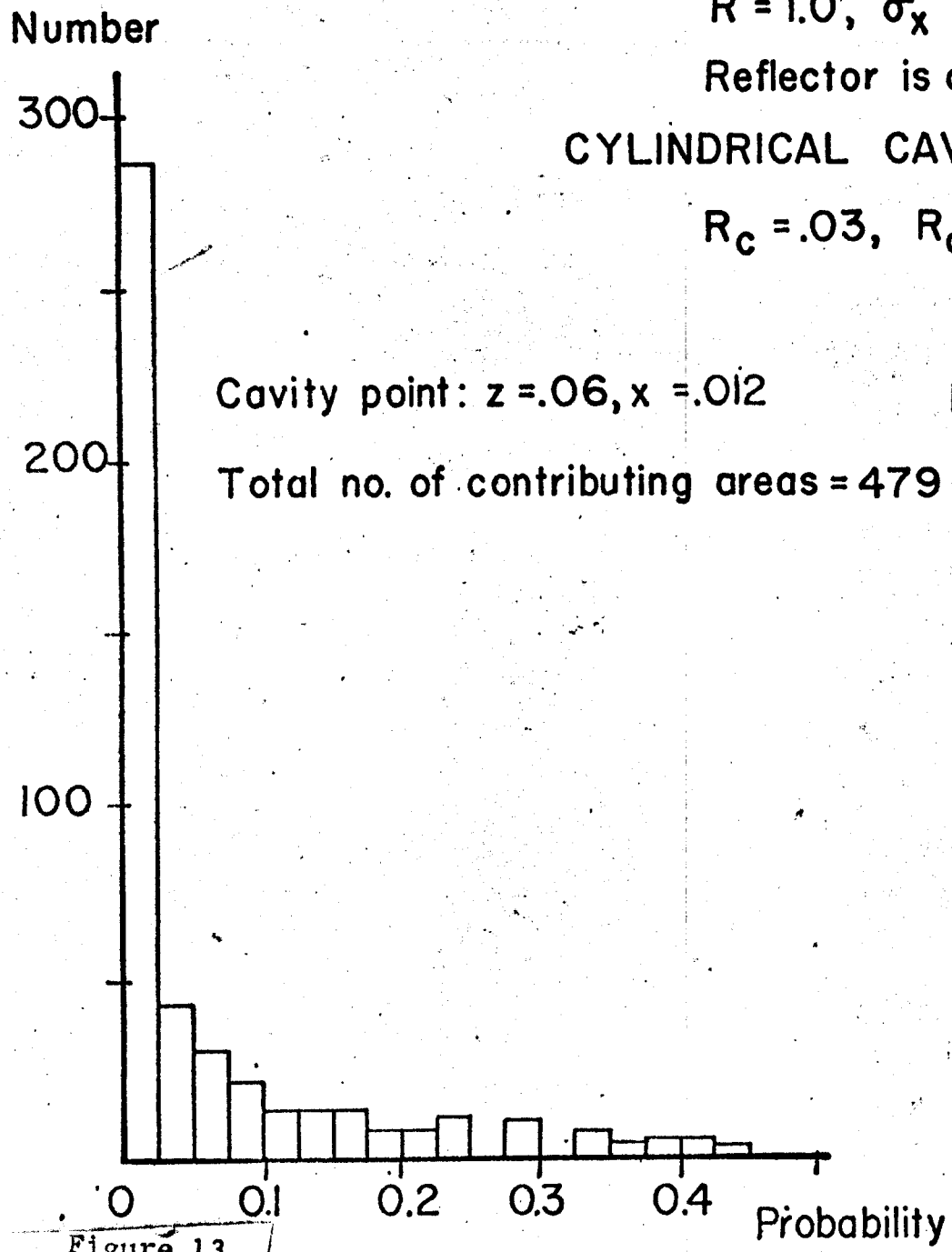

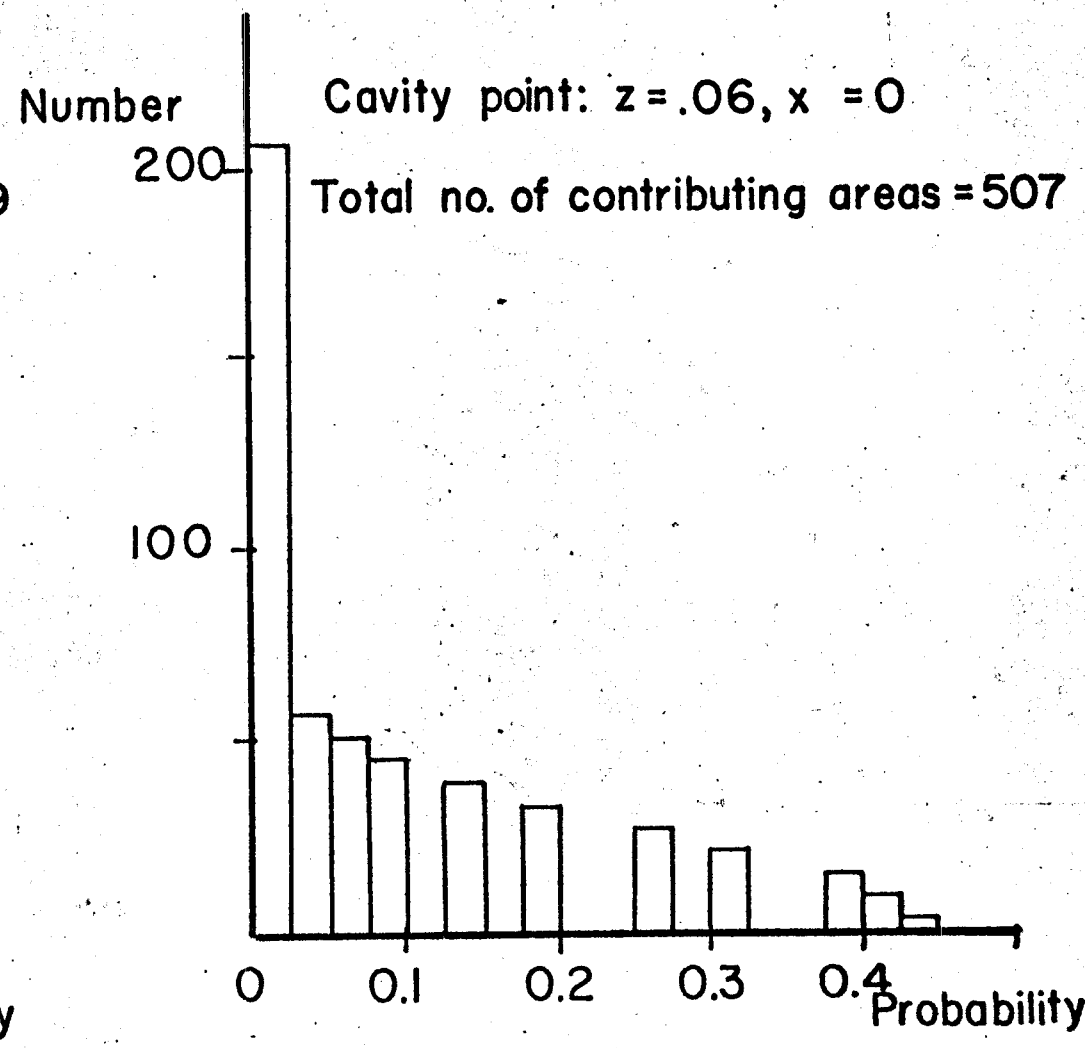

Figure 13

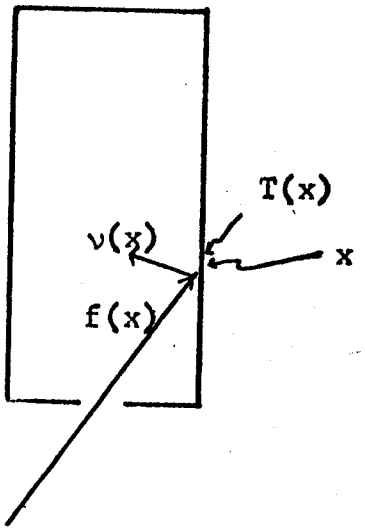

$$\nu(x) = \epsilon\sigma T^4(x) + (1 - \alpha)\left(f(x) + \int_{\substack{\text{walls}\\ \text{of the}\\ \text{cavity}}} K(x,x')\nu(x')dx' \right)$$

Figure 14

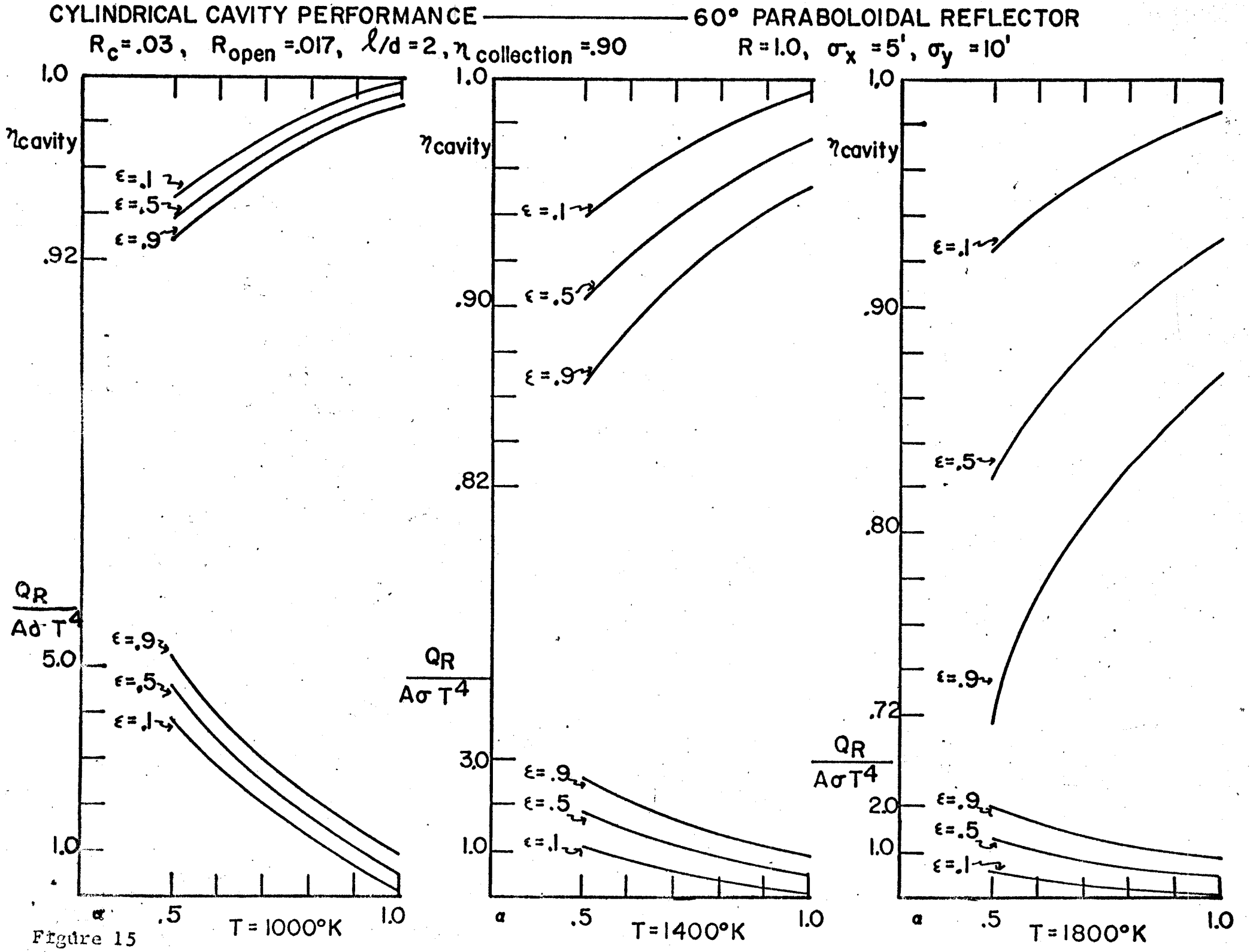
CYLINDRICAL CAVITY PERFORMANCE
$R_c = .03$, $R_{open} = .017$, $\ell/d = 2$, $\eta_{collection} = .90$
60° PARABOLOIDAL REFLECTOR
R = 1.0, $\sigma_x = 5'$, $\sigma_y = 10'$
η_{cavity}
1.0
.92
.90
.82
.80
.72
$\epsilon = .1$
$\epsilon = .5$
$\epsilon = .9$
$\frac{Q_R}{A\sigma T^4}$
5.0
3.0
2.0
1.0
0
.5
1.0
T = 1000°K
T = 1400°K
T = 1800°K

Figure 15

CAVITY PERFORMANCE

CYLINDRICAL CAVITY

$R_c = .03$

$R_{open} = .006$

$\ell/d = 2$

$\eta_{collection} = .90$

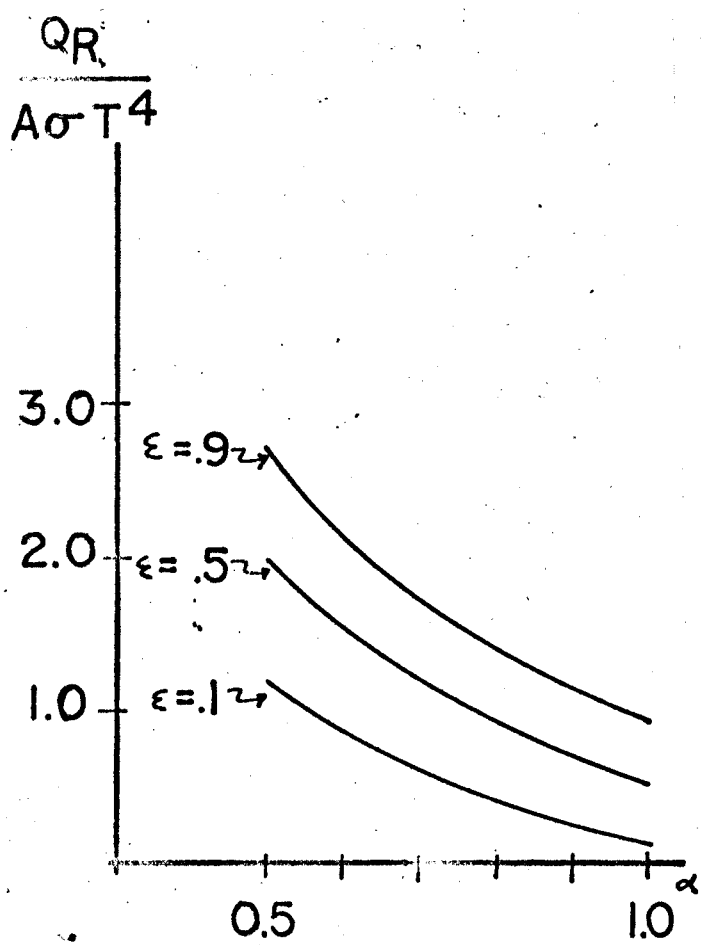

60° PARABOLOIDAL REFLECTOR

$R = 1.0$

$\sigma_x = 0$

$\sigma_y = 0$

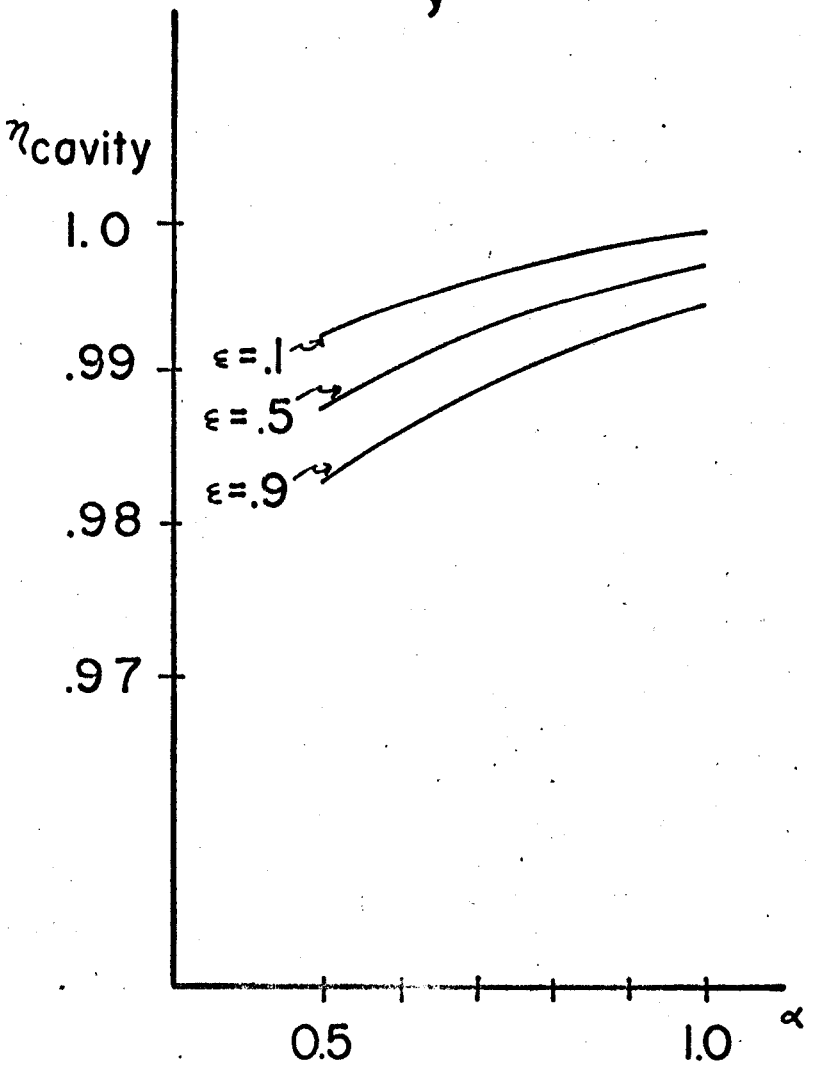

$T = 1400°K$

Figure 16